This is to certify that the

thesis entitled

ON ACCURACY ESTIMATES
FOR FINITE ELEMENT EIGENVALUE COMPUTATIONS

presented by

Yun-Jae Kim

has been accepted towards fulfillment
of the requirements for

M.S. degree in Mechanical Engineering

A. DIAZ
Major professor

Date 5-30-90

ON ACCURACY ESTIMATES FOR FINITE ELEMENT EIGENVALUE COMPUTATIONS

By

Yun-Jae Kim

A THESIS

Submitted to
Michigan State University
in partial fulfillment of the requirements
for the degree of

MASTER OF SCIENCE

Department of Mechanical Engineering

1990

ABSTRACT

ON ACCURACY ESTIMATES FOR FINITE ELEMENT EIGENVALUE COMPUTATIONS

By

Yun-Jae Kim

Accuracy estimates for finite element computations of elliptic eigenvalue problems are presented. From results of error estimates for elliptic boundary value problems, error estimates for elliptic eigenvalue problems are established for each mode based on interpolation error theory. An error indicator, which is defined as an element-wise approximation to the true error, is computationally implemented using two different techniques, a smoothing technique and a direct substitution technique using a differential operator. The accuracy of error indicators is checked using the eigenvalue problems of a uniform, Bernoulli-Euler beam. Two measures of accuracy are discussed. The first measures how accurately the estimator can capture the maximum true element-wise error over all elements. The second measures how accurately the estimator estimates the distribution of true error over the domain. Using the simple node-moving algorithm, improved grids are constructed keeping the total number of degrees of freedom constant.

ACKNOWLEDGEMENTS

The author would like to express his deepest gratitude to his advisor, Prof. A. Diaz, for his valuable guidence, encouragement during his years at MSU.

The author also feels highly indebted and would like to express his most sincere gratitude to his family, especially to his father, Tae-sup Kim, and to his mother, Kun-ja Hong Kim.

The author would like to thank other Korean students in ME Dept. at MSU, Keun-Chul Lee, Moon-suk Seo, Seoung-chool Yoo, Seung-bok Choi, Jung-ki Lee and Sang-woo Kim, for their help and friendship.

Finally, the author wish to give special thanks to Ji-young Sung and his wife, Hae-jung Park Sung, for their support and friendship during these years at MSU.

TABLE OF CONTENTS

1 Introduction 1

2 Review of Adaptive Finite Element Methods 4

2.1 Adaptive Methodology 4

2.2 Error Measurement 5

2.2.1 Residual Error Estimates 5

2.2.2 Error Estimates based on Interpolation Error 8

2.3 Adaptation Strategies 10

2.3.1 Elliptic Problems 11

2.3.2 Eigenvalue Problems 16

2.3.3 Time Dependent (Parabolic and Hyperbolic) Problems 17

3. Eigenvalue Problems and Finite Elements 20

3.1 Solutions in Infinite Dimensional Space 20

3.1.1 Differential Form 20

3.1.2 Weak (Variational) Form 23

3.2 Approximations in Finite Dimensional, Finite Element Subspaces 27

3.3 Summary 31

4 Error Indicators for Elliptic Eigenvalue Problems 32

4.1 Review of the Error Estimates for Elliptic Boundary Value Problems 32

4.2 Error Estimates for Elliptic Eigenvalue Problems 35

4.3 Error Estimators 37

4.4 Computational Implementation of Error Indicators 39

4.4.1 Smoothing Techniques 39

4.4.2 Direct Substitution Technique using a Differential Operator 42

4.5 Accuracy of Error Indicators 44

4.5.1 Accuracy on Maximum Errors 46

4.5.2 Accuracy on Error Distributions 61

4.5.3 Node Relocation : An Improved Grid 74

5 Conclusions and Recommendations 88

5.1 Conclusions 88

5.2 Discussions and Future Research 89

List of References 92

Appedices

A Mathematical Background 96

A.1 Real Linear Space 96

A.2 The Continuity Class $C^m(\Omega)$ 97

A.3 The $L^2(\Omega)$ class 98

A.4 The Sobolev Class $H^m(\Omega)$ 98

A.5 Equivalence of Two Norms 98

B Interpolation Functions for Quintic Beam Elements 100

B.1 Quintic Element Type 1 (3 nodes, 2 dof/node) 100

B.2 Quintic Element Type 2 (2 nodes, 3 dof/node) 101

C Exact Eigenpairs of a Uniform, Bernoulli-Euler Beam 103

C.1 Pinned-Pinned Beam (SS-SS) 103

C.2 Clamped-Free Beam (CL) 104

C.3 Clamped-Pinned Beam (CL-SS) 104

C.4 Clamped-Clamped Beam (CL-CL) 104

C.5 Normalization 106

LIST OF FIGURES

Figure 1.1 Approximation error in elliptic boundary value problems (measured in the energy norm) 33

Figure 1.2 Approximation error in elliptic eigenvalue problems (measured in the energy norm) 36

Figure 2. Relative percentage error in eigenvalue vs. Number of cubic beam elements 48

Figure 3.1 Error in eigenfunction vs. Number of cubic beam elements (pinned-pinned boundary condition) 50

Figure 3.2 Error in eigenfunction vs. Number of cubic beam elements (clamped-free boundary condition) 51

Figure 3.3 Error in eigenfunction vs. Number of cubic beam elements (clamped-pinned boundary condition) 52

Figure 3.4 Error in eigenfunction vs. Number of cubic beam elements (clamped-clamped boundary condition) 53

Figure 4. Relative percentage error in eignevalue vs. Number of quintic beam elements 56

Figure 5.1 Error in eigenfunction vs. Number of quintic beam elements (pinned-pinned boundary condition) 57

Figure 5.2 Error in eigenfunction vs. Number of quintic beam elements (clamped-free boundary condition) 58

Figure 5.3 Error in eigenfunction vs. Number of quintic beam elements (clamped-pinned boundary condition) 59

Figure 5.4 Error in eigenfunction vs. Number of quintic beam elements (clamped-clamped boundary condition) 60

Figure 6. Percentage error vs. Location along the beam (cubic beam element) 64-69

Figure 7. Percentage error vs. Location along the beam (quintic beam element) 71-73

Figure 8. Error in eigenvalue and eigenfunction vs. Nodal position 78-79

Figure 9. Error distribution of uniform and improved grid ..81-85

Figure 10. Nodal location of the improved grid 86

CHAPTER I.

INTRODUCTION

The finite element method has become an effective and powerful tool for obtaining approximate solutions to engineering problems. Much of the power of the method is due to the freedom that it allows in the construction of the discretized model. However, the quality of the finite element approximation greatly depends on how the discretization is performed. For this reason, in the last ten years considerable effort has been devoted to adaptive finite element methods which are designed to automatically improve the quality of the finite element approximation. The goal of adaptive finite element methods can be achieved only after computationally useful measures of the 'quality' of the approximation are available. This thesis discusses the construction of such measures for the simple class of 1-D eigenvalue problems.

In finite element methods, two basic techniques for error estimation have emerged : one based on residual error estimates, introduced by Babuska and Rheinbolt [1-4] and another based on interpolation error, introduced by Diaz et.al.[14-16]. The first class of error estimates is constructed from estimates of $\mathcal{L}(u-u^h)$,

where $\mathcal{L}$ denotes a differential operator and u and u^h are the solution sought and its approximation. The second technique is based on interpolation error theory and is constructed from an estimation of higher order derivatives of u.

Having resolved the issue of error estimation, one can improve the quality of finite element approximations efficiently using local refinement or relocation. In local refinement, more degrees of freedom are added to elements where the approximation is of lower quality by either increasing the order of polynomial approximation inside elements (p-method) [7] or by subdividing elements (h-method) [1-5]. In node relocation, the quality of the approximation is improved by optimizing the disposition of the nodes while keeping the number of degrees of freedom constant [14-16].

This thesis presents accuracy estimates for finite element computations of elliptic eigenvalue problems. From results of error estimates for elliptic boundary value problems, error estimates for elliptic eigenvalue problems are established for each mode based on interpolation error theory. An error indicator, which is defined as an element-wise approximation to the true error, is computationally implemented using two different techniques, a smoothing technique and a direct substitution technique using a differential operator. The accuracy of error indicators is checked using the eigenvalue problem of a uniform, Bernoulli-Euler beam. Two measures of accuracy are discussed. The first measures how accurately the estimator can

capture the maximum true element-wise error over all elements. The second measures how accurately the estimator estimates the distribution of true error over the domain. Using the simple node-moving algorithm proposed by Diaz et.al.[14-16], improved grids are constructed keeping the total number of degrees of freedom constant.

The thesis is divided into five chapters. Chapter two is a review of existing adaptive finite element methods. Error measurement techniques and adaptation strategies are reviewed with an emphasis on elliptic problems. Chapter 3 presents an overview of the solution to eigenvalue problems in infinite dimensional space and their approximation in finite element subspaces. In chapter 4, error estimates for elliptic boundary value problems are reviewed and error estimates for elliptic eigenvalue problems are established. As a computable form, two types of error indicators are proposed and their accuracy is tested. Node relocation is also performed to achieve an improved grid. Chapter 5 discusses the results of the research, presents conclusions and proposes further research.

CHAPTER II.

REVIEW OF ADAPTIVE FINITE ELEMENT METHODS

2.1 Adaptive Methodology

The objective of adaptive finite element methods is to adaptively change the finite element model to improve the quality of the finite element approximation.

A possible approach to improve the finite element solution is to increase the number of degrees of freedom by subdividing or increasing the degree of polynomial approximation. For example, new degrees of freedom can be added selectively to elements where the finite element approximation is poorer. In these elements, new degrees of freedom are added by subdividing the element or by increasing the degree of polynomial approximation within the element. This process can be repeated until a prescribed accuracy is achieved. We will refer to this process of selective addition of new degrees of freedom as optimal refinement. Another approach to improve the quality of the finite element solution is to relocate the mesh by reducing or increasing the element size (length in 1-D or area in 2-D) to achieve the best possible grid for the given number of degrees of freedom. This method can be referred to as optimal relocation problem. Both

the refinement and relocation approaches need the element information from previous solutions to decide where the approximation is poorer so as to add new degrees of freedom selectively.

To implement an adaptive strategy, one must address the following issues :

1. How to measure the quality of the approximation. The quality of the approximation is measured by the difference between the exact solution and the finite element approximation. There are two basic techniques to estimate errors in finite element analysis: the residual approach and the interpolation approach.

2. How to adapt the solution procedure to improve the quality of the approximation once an element-wise estimate of the error is known. Three methods are available involving refinement (h-method, p-method) and relocation (r-method). Combinations (such as h-p method) are also available.

We outline in the following section existing approaches to adaptive finite element methods and present a review of the adaptive finite element literature.

2.2 Error Measurement

2.2.1 Residual Error Estimates

One popular way to estimate the finite element error is the so-called residual error estimate technique. Consider the linear, elliptic differential equation.

$$\mathcal{L}\, u + q = 0 \quad \text{in } \Omega \tag{2.1}$$

with boundary conditions on $\partial\Omega$

Replacing u by its finite element solution u^h, one has

$$\mathcal{L}\, u^h + q = r \quad \text{in } \Omega \tag{2.2}$$

where r is the residual. It is assumed that the approximation u^h satisfies the boundary conditions. If the approximation u^h is exact, the residual r is zero. Otherwise, denoting the finite element error as $e=u-u^h$, subtracting (2.2) from (2.1) leads to

$$\mathcal{L}\, e = -\mathcal{L}(u-u^h) = -r$$

To measure an element-wise error, a local auxiliary problem must be solved, stated as follows :

$$\mathcal{L}\, w + q = 0 \qquad \text{in element K} \tag{2.3}$$

$$w = u^h \qquad \text{on element boundary } \partial K$$

In element K, the solution w to (2.3) is treated as the true solution. The element-wise residual, r_K, and the element-wise error in the energy norm, $||e^*||_{E,K}$, where $e^*=w-u^h$, can be defined as

$$r_K = [\mathcal{L}(w-u^h)]_K \qquad \text{and}$$

$$||e^*||^2_{E,K} = \int_K (w-u^h)\, r_K\, dK = \int_K (w-u^h)\mathcal{L}(w-u^h)\, dK \tag{2.4}$$

Integration by parts using the boundary condition of the local auxiliary problem leads to the final form of the element-wise error. For example, in a 1 dimensional 2nd order differential equation,

$$\frac{d^2u}{dx^2} + q = 0 \qquad \mathcal{L} = \frac{d^2}{dx^2} \qquad \text{in } \Omega \tag{2.5}$$

the local auxiliary problem associated with (2.5) is

$$\frac{d^2w}{dx^2} + q = 0 \qquad \text{in element K} \tag{2.6}$$

$$w = u^h \qquad \text{on element boundary } \partial K$$

The element-wise error in the energy norm is

$$||e^*||^2_{E,K} = \int_K e^* \frac{d^2e^*}{dx^2}\, dK = \int_K (w-u^h) \frac{d^2(w-u^h)}{dx^2}\, dK$$

Note that we have the boundary condition, $w-u^h = e^* = 0$ on ∂K

Integration by parts leads to the final form

$$||e^*||^2_{E,K} = \int_K [\, \frac{d}{dx}(w-u^h)\,]^2 dK \tag{2.7}$$

In general, the solution w to the local auxiliary problem (2.3) cannot be computed exactly and, instead, only an approximation w^* to w can be computed. There are several ways to compute the approximation w^*. For example, one may increase the polynomial degree of approximation inside K or, instead, one may refine the element K by subdividing it into smaller elements. Once the approximation w^* to w is available, the error in element K can be computed from eq (2.4).

The residual approach is complicated by difficulties in solving the local auxiliary problem. In addition, the approach is difficult to extend to nonlinear problems and to choose the appropriate norm. For a discussion of these difficulties, see Oden et.al. [27].

2.2.2 Error Estimates based on Interpolation Error

A different technique for error estimation, interpolation error theory, can be used to construct error estimates for adaptive finite elements. This approach was proposed by Diaz et.al. [14,15,16]. The procedure is outlined below.

Assume that the true solution u to an ordinary differential equation is a smooth function, and let u_I be an interpolator of u in a finite dimensional space. By construction. u_I is equal to u at the finite element nodes, i.e.,

$$u_I(b_j) = u(b_j) \tag{2.8}$$

where b_j are finite element nodes (j=1,2,...,NO) and NO is a number of nodes in the finite element model. When u is the solution to an elliptic boundary value problem, the error of approximating u by its finite element solution u^h is bounded by the error associated with the interpolation u by u_I. This follows from Cea's Lemma [45].

$$||u-u^h|| \leq c_1||u-u_I|| \quad \text{where } c_1 \text{ is a positive constant} \tag{2.9}$$

The following result is available from interpolation error theory :

$$||u-u_I||_{m,K} \leq c_2 \, h_K^{k+1-m} |u|_{k+1,K} \qquad (2.10)$$

where m, k and h_K denote the order of the variational form, the degree of the finite element solution and the diameter (length) of element K, respectively, and c_2 is a positive constant.

From (2.9) and (2.10),

$$||u-u^h||_{m,K} \leq c \, h_K^{k+1-m} |u|_{k+1,K} \qquad (2.11)$$

Inequality (2.11) provides the basis for element error estimates. For example, consider the solution u to a 2nd order differential equation approximated by the piecewise linear function u^h (k=1, m=1). The inequality (2.11) becomes,

$$||u-u^h||_{1,K} \leq c \, h_K \, |u|_{2,K}$$

This technique is simpler conceptually as well as computationally than the residual technique. However, when we use this technique, we face one problem: since the true solution u is, in general, not available, we have to use available information, the finite element solution, to estimate it. To estimate the error, we need to calculate higher order derivatives of u since the term $|u|_{k+1,K}$ includes (k+1)th order derivatives. However, the finite element solution u^h on element K is a k-th order polynomial. The procedure to extract higher order derivatives needs very accurate post-processing for error estimations. A simple technique was proposed by Diaz et.al. [14-16], and is also

used in the present work. A different technique based on rigorous estimates was proposed by Babuska and Miller [6], and extended by Demkowicz et.al.[5].

Applications of error estimation techniques based on both residual and interpolation approaches to linear problems in elasticity, fluid, and heat transfer as well as nonlinear problems can be found in the paper by Oden et.al. [27].

2.3 Adaptation Strategies

Suppose that we have already estimated the element-wise error of the approximation. We are now in position to change the finite element model in order to improve the accuracy of the approximation. The methodology for adaptation can be roughly classified into two classes : local refinement and relocation.

refinement

Local refinement increases the total degrees of freedom in the finite element model by

1. increasing the number of elements while keeping the polynomial degree of local basis functions fixed (h-method),or
2. increasing the polynomial degree of approximation while keeping the number of elements fixed (p-method)

node relocation

In the node relocation method (r-method), the total number of degrees of freedom remains constant. Nodes are relocated within a fixed number of elements and with a fixed polynomial degree of approximation. In time-dependent problems, some moving mesh methods (e.g. moving finite element method) have been proposed. These methods have similar basic features to the r-method.

combination

Some combinations of the above methods are possible (e.g. h-p, h-r, and p-r method). The most popular method is the combination of h and p method. (h-p method)

In the following sections, the different adaptation strategies are discussed based on the type of differential equation : time-independent (elliptic) and time-dependent (parabolic, or hyperbolic) problems. We also include discussion of eigenvalue problems, which are the main objective of this work.

2.3.1 Elliptic Problems

Since the late 70's, adaptive finite element methods have been applied to linear, elliptic problems, using heuristic as well as rigorous mathematical justifications. Originally developed for linear elliptic problems, adaptive finite element methods have now been extended to some classes of nonlinear problems. We review adaptive methods in elliptic problems based on the h-, p-, h-p, and r-method.

2.3.1.1 h-version

In the h-method, elements are subdivided into smaller ones while the order of polynomial approximation remains unchanged. Optimally refined meshes are achieved by selectively subdividing elements where the error is large until a specified accuracy is achieved. This method is based on the fact that, as the mesh size h goes to 0 (as the number of elements increase), the error in the energy converges to 0 [44]. The computational detail of this approach can be found in series of papers by Babuska and Rheinbolt [1-4], where the residual technique was used for error estimation. There, error indicators constructed from the finite element solution were used to identify elements where the approximation is less accurate.

An impressive work using the h-version of mesh refinement was done by Demkowicz et.al.[5], where interpolation error estimates are used to estimate the error and the extraction formula was modified to calculate highly accurate higher order derivatives.

2.3.1.2 p-version

In the p-method, the number of finite elements remains unchanged, while the order of polynomial approximation is selectively increased. The p-version of the finite element method is based on the notion that higher order polynomials can approximate a smooth function better than lower order ones. Distributing different higher order polynomials in regions where the approximation is poorer can produce better overall approximations. The higher order polynomial is used in the elements

where the error is large. Note that the original grid (element size) is not modified. The p-version was studied by Babuska et.al. [7]. The authors obtained error estimates in terms of the polynomial of degree p, and showed that if the convergence rate of the h-method and p-method is expressed in terms of the number of degrees of freedom, the p-method cannot have a slower rate of convergence than the h-method. In particular, when corner singularities are present, the convergence rate of the p-method is exactly twice that of the h-version. Numerous works have been published on p-methods, especially applications to fracture mechanics problems (see references in Szabo [10]) The p-method has been shown to produce better results than the h-method in elasticity problems with singularities. [7,11,12]

A popular way to formulate the p-version is the so called hierarchical finite element approach. This is a computationally efficient procedure in which the stiffness matrix corresponding to the hierarchically enriched mesh includes the stiffness matrix corresponding to the previous mesh as a submatrix. The hierarchical finite element method is discussed by Zienkiewicz et.al. [8,9]. The paper by Zienkiewicz and Craig [11] includes recent advances in the p-method and hieriarchical finite elements.

2.3.1.3 Combined h-p method

Babuska and Dorr [13] studied the combination of h and p-methods, where error estimates in terms of both the mesh size h and the polynomial degree p were explicitly obtained. An important result

there is that the optimal h-type refinement together with properly distributing p's can produce exponential convergence.

In summary, it is generally believed that a faster increase in local accuracy can be achieved using the p-method, specially in problems with singularities. The best approach in terms of accuracy is the combined h and p method, which leads to exponential convergence. These results have been restricted to one-dimensional problems and to linear elliptic problems in two dimensions.

2.3.1.4 r-version

The h- and p-method improve the finite element approximation by increasing the number of degrees of freedom. In some problems, however, one may want to keep the number of degrees of freedom constant, i.e. improve an existing grid. This is the case, for instance, when finite elements are used as part of an iterative design optimization process. In this context, the r-method was proposed by Diaz et.al. [14-16]. The paper [15] includes some theoretical aspects of the r-method. The work is summarized as an optimal relocation problem where an objective function B is derived based on interpolation error estimates and design variables are element lengths h in 1-D problems or areas A in 2-D problems. The optimal relocation problem is stated as follows :

(1) 1-dimensional case

Find the vector of element lengths $h=(h_1,h_2,\ldots,h_N)$ that

$$\text{minimizes } B^2(u,h) = \sum_{N=1}^{N} h_K^{2k} |u|^2_{k+1,K} \qquad (2.12.a)$$

$$\text{subject to } \sum_{K=1}^{N} h_K = 1 \quad , \quad h_K \geq 0$$

(2) 2-dimensional case

Find the vector of element areas $A=(A_1, A_2, \ldots, A_N)$ that

$$\text{minimizes } B^2(u,A) = \sum_{K=1}^{N} A_K^k \, |u|^2_{k+1,K} \qquad (2.12.b)$$

$$\text{subject to } \sum_{K=1}^{N} A_K = 1 \quad , \quad A_K \geq 0$$

where N is the total number of elements. The authors also derived optimality conditions for (2.12),

$$f_K = h_K^{2k} |u|^2_{k+1,K} = \text{constant} \quad \text{in 1 dimensional problems} \qquad (2.13.a)$$

$$f_K = A_K^k \, |u|^2_{k+1,K} = \text{constant} \quad \text{in 2 dimensional problems} \qquad (2.13.b)$$

for all $K=1,2,3,\ldots,N$. This means that the necessary condition for optimality of the grid-relocation problem is that the element-wise quantity f_K be the same for all elements $K=1,2,\ldots,N$. This grid is defined as an optimal grid. A simple node-moving algorithm was proposed to obtain the optimal grid. and successfully tested in [14,15,16]. This algorithm is also used in the present work. The r-method has proven to be effective for nonlinear problems (e.g. plasticity) in solid mechanics. and has been applied to fracture mechanics problems [14,15,16] as well as fluid mechanics problems [15]. The r-method can be more easily extended to time-dependent problems than the h and p versions.

Other applications of the h- and r-method (e.g.,in metal forming, flow problems and shape optimization) are referred to in the review paper by Kikuchi [17]. A general review of adaptive methods can be found in the paper by Oden et.al.[27].

2.3.1.5 Adaptive Mesh Generation Techniques

Adaptive mesh generation techniques which combine numerical grid-generation and adaptive finite element methods have also appeared in the literature [17]. Demkowicz and Oden [5] proposed a new mesh generation technique, which extends an existing conformal map-type mesh generator combined with a minimization of interpolation error estimates as the mesh modification strategy. Another mesh generation technique was presented in [19], where the h-type mesh refinement was adopted for mesh modification.

2.3.2 Eigenvalue Problems

In static, force-deflection (elasticity) problems, only one single solution is sought. For these problems, it has been statedin the previous section that the p-version is more attractive than the h-version. By contrast, in eigenvalue problems, a large number of solutions (eigenpairs associated with natural modes) are sought. In the paper by Bennighof and Meirovitch [20], two questions were

addressed regarding the convergence of finite element methods applied to eigenvalue problems : 1. Why the approximation to the eigenvalue and eigenfunction of the higher mode is poorer than that of the lower mode. 2. Why the p-method can produce significantly better eigenvalue convergence than the h-method. The authors also explain why the upper half of the modes obtained from finite element approximations are useless. The second issue is also discussed in the paper by Sun and Hwang [48], where higher order (quintic) elements were shown through numerical examples to be more efficient for beam-like structural dynamics problems. Error indicators based on p-version hierarchical adaptive finite element methods for eigenvalue problems were derived by Friberg in [21] and tested in [22]. The author has shown the superiority of the p-version through the observation that three-quarters of the lower mode eigenpairs are acceptable in the p-version, whereas only one-half of the lower mode eigenpairs are acceptable in the h-version for the same number of degrees of freedom.

2.3.3 Time Dependent (Parabolic and Hyperbolic) Problems

Recently, there have been significant advances in adaptive finite element methods applied to time dependent problems. For example, in computational fluid mechanics or in heat transfer problems governed by nonlinear partial differential equations, important features tend to occur in localized regions whose location may change

in time. The use of extremely fine meshes over the whole domain to capture these features accurately is not computationally feasible in realistic problems. In such problems, adaptive methods, especially moving-mesh methods, are very effective.

Miller and Miller [23] and Miller [24] proposed a Moving Finite Element (MFE) method for problems characterized by nonlinear partial differential equations such as Burger's equation with a large Reynolds number, which develop shocks and other sharp moving fronts. In the MFE method, the nodes are allowed automatically to concentrate and move with the front, making it possible to handle such problems with far fewer nodes and with larger time steps for time integration. The basic idea of the MFE method is that the approximation is a function of amplitudes as well as nodal positions, whereas it is only a function of amplitudes in usual FEM. Recent results and additional references are summarized in Miller [25].

Another moving-mesh method was proposed by Adjerid and Flaherty [24] for the class of 1 dimensional, 2nd order parabolic partial differential vector systems. The authors derived the error indicator based on residual estimates. The p-type mesh refinement was used to solve the local auxiliary problem. A differential equation was proposed to control the mesh motion so that three differential equations for approximation, error, and mesh motion control are solved concurrently.

Some important works have been done recently with applications in supersonic gas dynamics and fluid mechanics [27-31]. In [27], Oden

et.al. applied both residual and interpolation error estimates to the Navier Stokes equation as a model problem of incompressible/viscous flow problems. A moving-grid algorithm for supersonic flow between moving bodies was proposed by Strouboulis et.al. [30] using Taylor-Galerkin finite element approximations, which can be applied to rotor-stator flow problems in turbomachinery [31]. More general classes of unsteady, inviscid/compressible flow problems were also studied by Oden et.al. [29], where an effective adaptive scheme was formulated using a Lax-Wendroff/ Taylor-Galerkin method for a time-dependent Euler equation. The authors use h-enrichment as well as r-moving mesh adaptive methods, and errors are estimated based on a residual approach in the time domain and on interpolation error estimates in the space domain.

CHAPTER III.

EIGENVALUE PROBLEMS AND FINITE ELEMENTS

3.1 Solutions in Infinite Dimensional Space

3.1.1 Differential Form

Consider a 1-dimensional beam in transverse vibration. Under the assumption of small deflections and rotations and neglecting shear and rotary inertia effects, the transverse displacement is governed by the Bernoulli-Euler equation

$$\frac{\partial^2}{\partial x^2}\left[E\ I(x)\ \frac{\partial^2 y(x,t)}{\partial x^2}\right] = -\ m(x)\frac{\partial^2 y(x,t)}{\partial t^2} \qquad (1)$$

$$t \geq 0\ ,\quad 0 < x < \ell$$

+ boundary conditions .

In equation (1), E, I(x), m(x) and ℓ denote Young's modulus, area moment of inertia about neutral axis, mass per unit length and beam length, respectively. The solution to equation (1) is a function of space x as well as time t. The assumption that the solution to (1) is separable in time and space, i.e. $y(x,t)=u(x)T(t)$, leads to the following two equations:

$$\frac{d^2}{dx^2}\left[E\,I(x)\frac{d^2u}{dx^2}\right] = \lambda\, m(x)u(x) \qquad 0 < x < \ell \qquad (2)$$

$$\frac{d^2T}{dt^2} + \lambda\, T(t) = 0 \qquad t \geq 0 \ . \qquad (3)$$

The scalars λ that produce nontrivial solutions of (2) are the <u>eigenvalues</u> and the associated solutions $u(x)$ are the <u>eigenfunctions</u>. The eigenvalue problem for the transverse vibration of the Bernoulli-Euler beam is, therefore, as follows.

Find the pair $(\lambda, u(x))$ such that

$$\frac{d^2}{dx^2}\left[E\,I(x)\frac{d^2u(x)}{dx^2}\right] = \lambda\, m(x)u(x) \qquad 0 < x < \ell \qquad (4)$$

+ boundary conditions .

When can one solve the equation (4) exactly? Solutions to this problem must satisfy all the boundary conditions as well as the differential equation in $0 < x < \ell$. The solution of (4) must be smooth so that u and its partial derivatives up to 4th order are continuous at every point in $(0,\ell)$. These are difficult conditions to satisfy. A small complication, such as a tapered cross section, can make (4) not solvable in closed form.

As another example, consider a 2-dimensional thin elastic plate in transverse vibration. The eigenvalue problem can be expressed as

$$\frac{\partial^4 u(x,y)}{\partial x^4} + 2\frac{\partial^4 u(x,y)}{\partial x^2 \partial y^2} + \frac{\partial^4 u(x,y)}{\partial y^4} = \lambda\, u(x,y) \qquad (x,y) \in \Omega \qquad (5)$$

+ boundary conditions on $\partial\Omega$.

In this case, we can get the general terms of the series solution only when the problem is defined over a simple domain. e.g. circular or rectangular with simple boundary conditions, e.g. clamped or simply supported along the boundary.

The general eigenvalue problem (including beam, plate etc) can be written in a compact form as follows .

Find the pair (λ,u), where $u \in C^{2m}$, such that

$$L\,u = \lambda\,u \quad \text{in } \Omega$$

$$M\,u = 0 \quad \text{on } \partial\Omega \qquad (6)$$

where L and M are linear differential operators and Ω is a smooth, bounded region with its boundary $\partial\Omega$. The differential operator L is a self-adjoint, elliptic operator of order 2m and M is a compatible boundary operator of order m. We will call equation (6) the differential form. Equation (6) has an infinite number of solution eigenpairs (λ,u) and since the equation is homogeneous in u, amplitudes of eigenfunctions are arbitary and only their shape can be determined uniquely.

Admissible boundary conditions are either essential, resulting from the geometric compatibilities, or natural, resulting from moment or shear force equilibrium. For example, in the case of the Bernoulli-Euler beam of length ℓ simply supported at both ends, boundary conditions are

essential : $u(0) = 0 \quad u(\ell) = 0$

$$\text{natural} \quad : \quad E\,I(0)\frac{d^2u(0)}{dx^2} = 0 \qquad E\,I(\ell)\frac{d^2u(\ell)}{dx^2} = 0 \quad . \tag{7}$$

In the case of the thin elastic plate clamped along its boundary $\partial\Omega$,

$$\text{essential} : \quad u(s) = 0 \quad \frac{\partial u(s)}{\partial n} = 0 \qquad s \in \partial\Omega \tag{8}$$

natural : none .

3.1.2 Weak (Variational) Form

The differential form (6) requires that u and all of its derivatives of order less than or equal to 2m be continuous at every point in Ω (i.e, u is in C^{2m}). This is a difficult condition to satisfy. A weak or variational formulation relaxes this requirement and facilitates computations. This weak form will be used to obtain a finite element approximation to the eigenfunction.

Consider again the differential form (4) and boundary conditions (7), representing the behavior of the Bernoulli-Euler beam simply supported at both ends. We multiply a weight (test) function v defined on $(0,\ell)$ to both sides of equation (4) and integrate over the domain such that the differential equation with boundary conditions is satisfied in the sense of weighted average, i.e.,

$$\int_0^\ell v \left[\frac{d^2}{dx^2} \left(EI(x) \frac{d^2u}{dx^2} \right) - \lambda u \right] dx = 0 \quad \text{in } (0,\ell)$$

$$+ \text{ boundary conditions} \quad \text{on } \partial\Omega \quad . \tag{9}$$

The equation (9) includes 4th order derivatives of u, whereas no derivatives of v appear. Integration by parts of (9) leads to

$$\int_0^\ell E\, I(x) \frac{d^2u}{dx^2} \frac{d^2v}{dx^2}\, dx - \lambda \int_0^\ell uv\, dx = 0 \qquad \text{in } (0,\ell), \quad (10)$$

provided that the solution u and the test function v belong to the class of admissible functions, denoted by V, defined as

$$V = \{\, v \in H^2 \mid v(0)=0,\ v(\ell)=0 \,\}$$

In words, V is the set of H^2-functions (bounded energy) that satisfy the essential boundary conditions $v(0)=0$ and $v(\ell)=0$. A function is said to be in H^2 if the function and all of its partial derivatives up to 2nd order are defined in a square-integral sense (see Appendix A for more detail), i.e.,

$$H^2 = \{\, v \mid |v|_0, |v|_1, |v|_2 \le M < \infty \,\} \quad .$$

where $|v|_0 = \int_0^\ell v^2 dx$, $|v|_1 = \int_0^\ell (\frac{dv}{dx})^2 dx$, $|v|_2 = \int_0^\ell (\frac{d^2v}{dx^2})^2 dx$ and M is a constant. Note that essential boundary conditions are included in the definition of V and that the smoothness requirement on u is weakened. Now we can write the weak form of this problem as follows :

Find $u \in V$ such that

$$\int_0^\ell E\, I(x) \frac{d^2u}{dx^2} \frac{d^2v}{dx^2}\, dx - \lambda \int_0^\ell uv\, dx = 0 \quad \text{for all } v \text{ in } V \qquad (11)$$

where V is defined as before.

In the case of the thin elastic plate clamped along its boundary, the weak form can be derived follwing similar steps. After introducing V and integrating by parts, the corresponding weak form is

find $u \in V$ such that

$$\int_\Omega \nabla^2 u \, \nabla^2 v \, dxdy - \lambda \int_\Omega uv \, dxdy = 0 \quad \text{for all } v \text{ in } V \qquad (12)$$

where ∇^2 is Laplacian operator defined by $\nabla^2 = \frac{\partial^2}{\partial x^2} + \frac{\partial^2}{\partial y^2}$.

The weak form can be written in a compact form by introducing inner products. The general form of variational eigenvalue problems is

find $u \in V$ such that

$$a(u,v) - \lambda(u,v) = 0 \quad \text{in } \Omega \qquad \text{for all } v \text{ in } V \qquad (13)$$

where $a(.,.)$ is a symmetric, bilinear energy inner product and $(.,.)$ is a symmetric, linear inner product.

In the case of the Bernoulli-Euler beam of length ℓ simply supported at both ends,

$$a(u,v) = \int_0^\ell E\, I(x) \frac{d^2u}{dx^2} \frac{d^2v}{dx^2} \, dx \ , \quad (u,v) = \int_0^\ell uv \, dx \qquad \text{in } \Omega(0,\ell)$$

u and v should satisfy $u(0) = v(0) = 0 \quad u(\ell) = v(\ell) = 0$.

In the case of the thin elastic plate.

$$a(u,v) = \int_\Omega \nabla^2 u \, \nabla^2 v \, dxdy \ , \quad (u,v) = \int_\Omega uv \, dxdy \qquad \text{in } \Omega$$

where $\nabla^2 = \frac{\partial^2}{\partial x^2} + \frac{\partial^2}{\partial y^2}$

u and v should satisfy $u(s)=v(s)=0$, $\frac{\partial u(s)}{\partial n}=\frac{\partial v(s)}{\partial n}=0 \quad s\in\partial\Omega$.

The differential form (6) and weak form (12) lead to an infinite number of eigenpairs (λ,u). These pairs can be ordered according to the magnitude of eigenvalues under the assumption of no repeated eigenvalues, i.e.,

$$\lambda_1< \lambda_2< \lambda_3< \ldots < \lambda_\ell< \ldots .$$

The eigenpair (λ_ℓ,u_ℓ) is the ℓ-th mode eigenpair. Equations (6) and (13) can be written in terms of the ℓ-th mode as follows.

differential form

Find the pair (λ_ℓ,u_ℓ) where $u_\ell \in C^{2m}$ such that

$$Lu_\ell = \lambda_\ell u \quad \text{in } \Omega$$

$$Mu_\ell = 0 \quad \text{on } \partial\Omega \qquad (6.a)$$

weak form

Find u_ℓ V such that

$$a(u_\ell,v) - \lambda_\ell(u_\ell,v) = 0 \quad \text{in } \Omega \quad \text{for all } v \text{ in } V \qquad (13.a)$$

General comments on this weak form should be made :

1. The solution u as well as the test function v belong to the class of admissible functions V defined as follows :

$V = \{ v\in H^m \mid v \text{ must satisfy essential boundary conditions} \}$

where m is the order of the weak (variational) form.

2. Assume that the solution to the weak form (13) is smooth enough. Then the weak form (13) and the differential form (6) are equivalent. See reference [43] for proof.

3. The weak form still cannot be solved in closed form. However, it is important in the sense that it will be used to derive useful finite element formulations.

Since, in general, neither the differential form nor the weak form can be solved in closed form, an approximation to u is needed. We discuss approximate solutions in finite dimensional subspaces next.

3.2 Approximations in Finite Dimensional, Finite Element Subspaces

We will approximate the weak solution within a finite-dimensional subspace V^h of the full admissible space V. In this subspace, the problem is stated as follows :

Find an approximated pair λ^h and u^h such that

$$a(u^h,v^h) = \lambda^h(u^h,v^h) \text{ for all } v^h \text{ in } V^h \subset V \qquad (14)$$

The approximation u^h on the subspace V^h has the form of $u^h = \sum_{i=1}^{N} q_i \phi_i$, where N is the dimension of V^h, q_i are unknown constants to be determined, and ϕ_i are linearly independent basis functions spanning

the subspace V^h. The finite element method provides a systematic technique for constructing the basis functions ϕ_i. In the finite element method, the basis functions ϕ_i are typically piecewise polynomials and are chosen in such a way that the parameters q_i are the values of u, and possibly its derivatives, at the nodal points.

Consider a 1-dimensional, 4th order problem in the domain $(0,\ell)$ such as a beam vibration problem. We discretize the domain into M finite beam elements, i.e., there are M elements and (M+1) nodes. Since V^h should be contained in V, the approximation u^h and the test function v^h must be in H^2 and satisfy essential boundary conditions. From the first requirement, $\frac{d^2u^h}{dx^2}$ must be square integrable, which does not allow discontinuities in $\frac{du^h}{dx}$. Thus in this problem the finite element basis function must be such that the function ϕ and its first derivatives are continuous throughout the domain. The simplest choice is the Hermite cubic polynomial that interpolates both the function value and its derivative over each element. The global basis function consists of two functions $\psi(x)$ and $\omega(x)$ so that the approximation u^h takes the form of

$$u^h(x) = \sum_{i=1}^{M+1} u_i^h \psi(x) + \sum_{i=1}^{M+1} \frac{du_i^h}{dx} \omega(x) \quad .$$

The Hermite cubic element has 2 degrees of freedom (the function value and its derivative) at each node, and hence there are 2(M+1) degrees of freedom in the finite element model. Thus N, the dimension of V^h, is 2(M+1). The global basis functions $\psi(x)$ and $\omega(x)$ have the following properties:

$$\psi_i(x_j) = \delta_{ij} \qquad \frac{d\psi_i(x_j)}{dx} = 0$$

$$\omega_i(x_j) = 0 \qquad \frac{d\omega_i(x_j)}{dx} = \delta_{ij} \qquad 1 \le i,j \le M .$$

In the finite element method, the approximation is constructed one element at a time, the final formulation being obtained by summing up the contribution of each element. Within element K, the restriction of u^h in element K is

$$(u^h)^K = \sum_{i=1}^{4} q_i^{(K)} \phi_i^{(K)} \tag{15}$$

where $\phi_i^{(K)}$(i=1,2,3,4) are local shape functions (cubic polynomial) in element K. Patching together shape functions ϕ_1, ϕ_3 and ϕ_2, ϕ_4 over the domain lead to the global basis function $\psi(x)$ and $\omega(x)$ respectively. The nodal values $q_1^{(K)}$ and $q_3^{(K)}$ represent the displacements at nodes i and i+1, and $q_2^{(K)}$ and $q_4^{(K)}$ represent the slopes at nodes i and i+1.

Substituting the element-wise approximation (15) and the test function into the weak form (14) leads to an element matrix,

$$[K]\ q = \lambda^h\ [M]\ q \qquad (16)$$

where [K] and [M] are the 4x4 element stiffness and mass matrix. Summing up the contribution of each element, one can get the global formulation,

$$[K]^G Q = \lambda^h\ [M]^G Q \qquad (17)$$

where $[K]^G$ and $[M]^G$ are the N by N global stiffness and mass matrix. Equation (17) is a matrix eigenvalue problem. The approximated eigenfunction u^h can be computed from the approximated eigenvector Q and global basis functions ϕ, i.e.,

$$u^h = \sum_{i=1}^{N} Q_i \phi_i \quad .$$

The matrix eigenvalue problem (17) leads to N approximated eigenpairs (λ^h, u^h). As before, ordering them according to the magnitude of approximated eigenvalues, i.e.,

$$\lambda_1^h < \lambda_2^h < \lambda_3^h < \ldots < \lambda_{N-1}^h < \lambda_N^h$$

the approximated eigenvalue λ_ℓ^h and corresponding eigenvector Q_ℓ are the ℓ-th mode eigenvalue and eigenvector The ℓ-th mode approximated eigenfunction u_ℓ^h can be computed from

$$u_\ell^h = \sum_{i=1}^{N} Q_{\ell i} \phi_i \quad .$$

Equation (17) can be also written in terms of the ℓ-th mode as follows.

$$[K]^G Q_\ell - \lambda_\ell^h [M]^G Q_\ell \qquad (17.a)$$

4.3 Summary and Discussion

In the previous sections, we have gone from the differential form (6,6.a) to the matrix eigenvalue problem (17,17.a). Closed form solutions to the differential form (6) or to the weak form (13) are not generally available, which leads to approximations in finite dimensional subspaces V^h of the original space V. We selected V^h as a finite element space. In general, V^h differs from V and the finite element approximation is different from the exact solution. Our concern is to reduce the error between the finite element approximation u^h and the exact solution u.

To reduce the approximation error, an <u>error indicator</u> should be constructed first so that we can estimate and reduce the error based on the error indicator. This question is discussed in the next chapter.

CHAPTER IV.

ERROR INDICATORS FOR ELLIPTIC EIGENVALUE PROBLEMS

4.1 Review of the Error Estimates for Elliptic Boundary Value Problems

Let u be the weak solution to the variational form of the elliptic boundary value problem of order m, $a(u,v)=(f,v)$ for all v in V, where V denotes an admissible space. Then u minimizes the functional (potential energy) $I(v)=a(v,v)-2(f,v)$ over V. Let u^h be a finite element approximation to this problem. Then u^h is the solution to $a(u^h,v^h) = (f,v^h)$ for all v^h in V^h, where V^h denotes a finite element subspace. It is also the minimizing function of the functional I(v) over V^h :

Theorem [44]

(a) $a(u-u^h,u-u^h) = \underset{v^h \text{ in } V^h}{\text{Min}} \; a(u-v^h,u-v^h)$ for all v^h in V^h

This means that, measured in the energy norm, u^h is the best possible member of all the members in the subspace V^h.

(b) $a(u-u^h,v^h) = 0$ for all v^h in V^h

The error $u-u^h$ is orthogonal to all the members in V^h, i.e., u^h is the projection of u onto the subspace V^h with respect to the energy inner product. See Figure 1.1.

The distance between u and u^h in the energy norm is bounded by

$$a(u-u^h,u-u^h) \leq c^2 h^{2(k+1-m)} |u|^2_{k+1} \qquad \text{for } u \in H^{k+1}(\Omega) \qquad (18)$$

where k is a polynomial degree of approximations in subspace V^h, c is a constant independent of h, m is an order of the variational form, $|.|_{k+1}$ denotes the semi-norm in $H^{k+1}(\Omega)$ and h is the size of the largest element.[44] In 1-D, h is the length of the largest element. In 2-D, h is the diameter of the largest circle inscribed in the largest element.

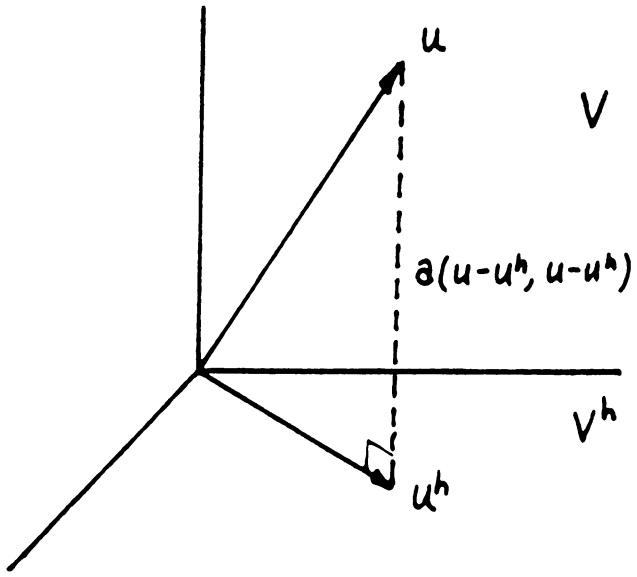

Figure 1.1
Approximation error in elliptic boundary value problems
(measured in energy norm)

The exponent of h in (18) indicates the rate of convergence as meshes are refined. The error can be reduced if h becomes smaller via mesh refinements : as $h \to 0$, $a(u-u^h, u-u^h) \to 0$. As more elements are used, the finite element solution u^h converges to the solution u in the energy norm. This is the key to the h-method.

The term $|u|_{k+1}$ reflects the smoothness of solution. Suppose that linear interpolation functions (k=1) are used to approximate the solution to the 2nd order elliptic problem (m=1). From (18), the approximation error is bounded by $c^2h^2|u|_2^2$ and the convergence rate in the energy norm is 2. If u is linear, the error is 0 since the $|u|_2$ term vanishes. This is the case in truss problems with concentrated loads. If u is quadratic, the approximation error is not 0 since the $|u|_2$ term does not vanish. However, if we used quadratic interpolation functions (k=2), the approximation error would be bounded by $c^2h^4|u|_3^2$ and, thus, the error would again be 0 since the $|u|_3$ term would vanish. Higher order basis functions can approximate u better. This is the key to the p-method.

Equation (18) is the key for the construction of error estimates for elliptic boundary value problems. The same equation will be applied to elliptic eigenvalue problems.

4.2 Error Estimates for Elliptic Eigenvalue Problems

In elliptic boundary value problems, the finite element approximation u^h is the projection of u onto V^h and is the closest member to u in V^h. However, in elliptic eigenvalue problems, the closest approximation to the ℓ-th mode eigenfunction u_ℓ in V^h is the Rayleigh projection Pu_ℓ. The Rayleigh projection Pu_ℓ is defined as follows :

If u_ℓ is the ℓ-th mode eigenfunction (solution) to the variational eigenvalue problem in V, then the Rayleigh projection Pu_ℓ is its orthogonal projection in the subspace V^h , i.e.,

$$a(u_\ell - Pu_\ell, v^h) = 0 \text{ for all } v^h \text{ in } V^h.$$

By definition, the Rayleigh projection Pu_ℓ is the closest approximation in V^h to u_ℓ measured in the energy norm. See Figure 1.2.

Since the projection of u_ℓ onto V^h is Pu_ℓ, the error bound (18) for elliptic boundary value problems suggests the following error bound for the ℓ-th mode eigenfunction u_ℓ for elliptic eigenvalue problems :

$$a(u_\ell - Pu_\ell, u_\ell - Pu_\ell) \leq c' h^{2(k+1-m)} |u_\ell|^2_{k+1} \quad . \tag{19}$$

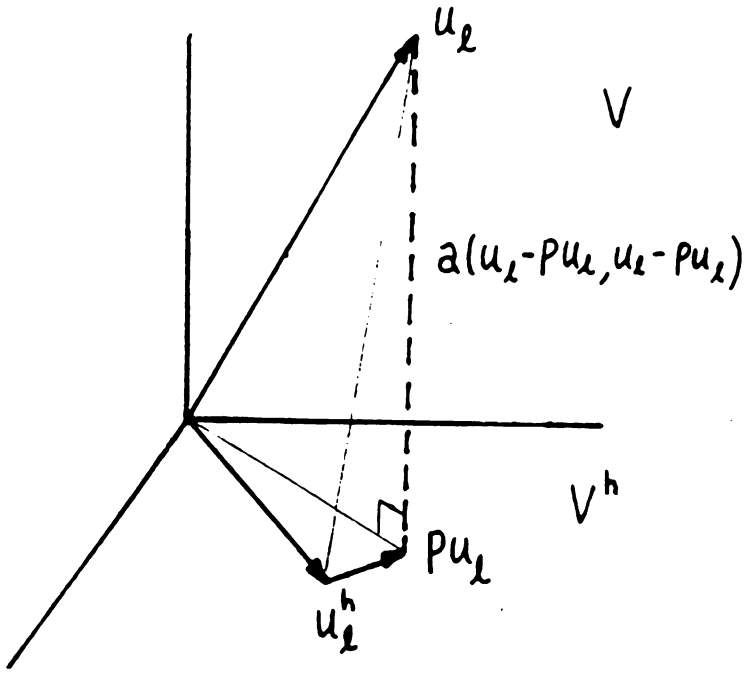

Figure 1.2 Approximation error in elliptic eigenvalue problems (measured in the energy norm)

Using the equivalence of the energy and H^m norm, equation (19) is equivalent to

$$||u_\ell - Pu_\ell||_m \leq ch^{k+1-m}|u_\ell|_{k+1} \tag{20}$$

where $||.||_m$ denotes the H^m norm (Sobolev norm).

The distance between u_ℓ and u_ℓ^h in the energy norm is expressed as

$$a(u_\ell - u_\ell^h, u_\ell - u_\ell^h) = a(u_\ell - Pu_\ell, u_\ell - Pu_\ell) + a(Pu_\ell - u_\ell^h, Pu_\ell - u_\ell^h) \ . \tag{21}$$

If V^h is a finite element space, the Rayleigh projection Pu_ℓ is not computable in general, but is 'close' to u_ℓ^h, i.e., $u_\ell^h \approx Pu_\ell$. Thus, if

the term $a(Pu_\ell - u_\ell^h, Pu_\ell - u_\ell^h)$ in (21) can be neglected, from (19) and (21),

$$a(u_\ell - u_\ell^h, u_\ell - u_\ell^h) \le c' h^{2(k+1-m)} |u_\ell|^2_{k+1} \quad . \tag{22}$$

This error bound (22) allows us to set up the explicit form of error estimators for eigenvalue problems.

4.3 Error Estimators

To improve the quality of approximations efficiently, new degrees of freedom should be added in a selective manner to elements where the approximation is poorer. This requires error information at the element level. Define an element-wise estimator of the true error as an error estimator and let ϵ_K^ℓ denote the error estimator of the ℓ-th mode in the element K. Then, the error bound (22) suggests the following form of the error estimator.

$$\epsilon_K^\ell = c\, h_K^{2\alpha} |u_\ell|^2_{k+1,K} \qquad \text{in 1-D} \tag{23.a}$$

$$\epsilon_K^\ell = c\, A_K^{\alpha} |u_\ell|^2_{k+1,K} \qquad \text{in 2-D} \tag{23.b}$$

where h_K is a length of element K,

A_K is an area of element K,

ℓ is a mode number,

k is the order of local basis functions,

α is the order of convergence (=k+1-m).

c is a constant independent of h_K, A_K and ℓ,

and $|.|_{k+1,K}$ denotes the H^{k+1} semi-norm on element K.

Note that the constant c depends only on the element type. In general, this constant is not available. For example, suppose that Hermite cubic interpolation functions (standard beam element, 2 nodes and 2 dof per node) are used to approximate solutions (eigenfunctions) to the vibration of a uniform, Bernoulli-Euler beam. Then the ℓ-th mode error estimator on element K is

$$\epsilon_K^{\ell} = c\, h_K^{2\alpha} |u|_{k+1,K}^2 = c\, h_K^4 \int_K \left(d^4 u_{\ell}/dx^4\right)^2 dx \qquad \alpha=2 \quad .$$

The error estimator of the form (23) is not still usable for computation since it includes the exact solution u_{ℓ}. To make the form (23) computable, it is necessary to replace u_{ℓ} by a known function that can be computed from the finite element approximation u_{ℓ}^h. Let $\hat{u}_{\ell}$ be such function. Then, the computable form of the error estimator, denoted by η_K^{ℓ}, is

$$\eta_K^{\ell} = h_K^{2\alpha} |\hat{u}_{\ell}|_{k+1,K}^2 \qquad \alpha=k+m-1 \quad . \qquad (24)$$

We call this an <u>error indicator</u>. The error indicator should be available from finite element approximations. Different forms of $\hat{u}$ will be discussed in the following sections. This is the main result of this work.

4.4 Computational Implementation of Error Indicators

Recall that the error indicator has the form of

$$\eta_K^{\ell} = h_K^{2\alpha} |\hat{u}_{\ell}|^2_{k+1,K} \qquad \alpha=k+m-1 \qquad (24)$$

The function $\hat{u}_{\ell}$ should be, first, computed easily from the finite element solution u_{ℓ}^h and, second, such that the ratio $|u_{\ell}-\hat{u}_{\ell}|_{k+1,K}$ / $|u_{\ell}|_{k+1,K}$ is small and asymptotically correct, i.e., converges to zero as $h \to 0$. In this section, two techniques to construct $\hat{u}_{\ell}$ are discussed.

4.4.1 Smoothing Technique

This technique was originally proposed and successfully tested by Diaz et.al. in [14,15,16]. Using this technique, the function $\hat{u}_{\ell}$ is constructed directly from the finite element approximation. For simplicity, let us illustrate only the 1-dimensional case here. In a 1-D problem, an approximation u_{ℓ}^h is a k-th order polynomial over each element where k is the polynomial degree of local basis functions. The k-th derivative of u_{ℓ}^h is a constant that may vary from element to element, and the (k+1)-th derivative vanishes inside the element and is undefined across elements. The new function $\hat{u}_{\ell}$ is defined such

that the difference between $\frac{d^k \hat{u}_\ell}{d x^k}$ and $\frac{d^k u_\ell^h}{d x^k}$ vanishes in the weighted average sense, i.e.,

$$\int_\Omega v \left(\frac{d^k \hat{u}_\ell}{d x^k} - \frac{d^k u_\ell^h}{d x^k} \right) dx = 0$$

where v is a weight function and k is the order of the basis functions of u_ℓ^h.

Let us illustrate the procedure using an example. Consider cubic beam elements over the domain $\Omega=(0,1)$. The approximation u_ℓ^h is a 3rd order polynomial on the element. Over the domain, the 3rd order derivative of u_ℓ^h is a piecewise constant function.

The function $\hat{u}_\ell$ satisfies

$$\int_0^1 v \left(\frac{d^3 \hat{u}_\ell}{d x^3} - \frac{d^3 u_\ell^h}{d x^3} \right) dx = 0. \tag{25}$$

To simplify the notation, let z_ℓ and p_ℓ be the 3rd order derivative of $\hat{u}_\ell$ and u_ℓ^h. Then eq (25) becomes

$$\int_0^1 v \left(z_\ell - p_\ell \right) dx = 0 \tag{26}$$

where p_ℓ is a constant since u_ℓ^h is a 3rd order polynomial. Choose linear basis functions for v and z_ℓ, i.e.,

$$v = \sum_{j=1}^{NO} \phi_j v_j \qquad z_\ell = \sum_{i=1}^{NO} \phi_i z_i \tag{27}$$

where NO is a number of finite element nodes, ϕ's are linear basis functions, and the vector z_i includes nodal values of z_ℓ.

Substituting (27) into (26) gives a system of equations,

$$\sum_{j=1}^{NO} A_{ij} z_j = b_i \quad , \quad i=1,2,\ldots,NO \tag{28}$$

$$A_{ij} = \int_0^1 \phi_i \phi_j \, dx \quad \text{and} \quad b_i = p_\ell \int_0^1 \phi_i \, dx \quad .$$

Eq (28) gives nodal values of a piecewise linear function z_ℓ.

When quintic beam elements are used, the procedure is the same except that now the function $\hat{u}$ satisfies

$$\int_0^1 v \left[\frac{d^5 \hat{u}_\ell}{dx^5} - \frac{d^5 u_\ell^h}{dx^5} \right] dx = 0 \quad .$$

Using this technique, the ℓ-th mode error indicator of element K has the form,

$$\eta_K^\ell = h_K^{2\alpha} |z_\ell|_{1,K}^2 = h_K^{2\alpha} \int_K (dz_\ell/dx)^2 dx.$$

We will call this type of indicator the <u>interpolation type 1 indicator</u>.

This smoothing technique can be easily extended to more general problems such as a tapered beam or two dimensional problems since the function $\hat{u}_\ell$ is constructed only from finite element approximations. On the other hand, this method has one defect: As more derivatives are taken of the finite element approximation, the accuracy may be

lost. The function u_ℓ^h may be very close to u_ℓ, but $d^3u_\ell^h/dx^3$ may not be close to d^3u_ℓ/dx^3. Therefore, the function $\hat{u}_\ell$ computed from $d^3u_\ell^h/dx^3$ may lack the necessary accuracy. More details about the accuracy of this type of indicator will be given in the next section using numerical examples.

4.4.2 Direct Substitution Technique using a Differential Operator

The term $|u_\ell|^2_{k+1}$ includes derivative terms of u_ℓ that may be replaced using a differential operator L. Recall the differential form of the eigenvalue problem $L\,u_\ell = \lambda_\ell\,u_\ell$. The basic motivation is to reduce the order of the derivative terms of u_ℓ. This technique is immediately applicable to only one case : a uniform, Bernoulli-Euler beam in 1-D. Let us illustrate the details using this case.

Consider the vibration of a uniform, Bernoulli-Euler beam governed by

$$L\,u_\ell = m\,\lambda_\ell u_\ell \quad , \quad L = E\,I\,\frac{d^4}{dx^4} \tag{29}$$

where E,I and m are constants. When cubic beam elements are used, the error estimator of the element K has the form

$$\epsilon_K^\ell = c\,h_K^4\,|u_\ell|^2_{4,K} \quad . \tag{30}$$

The term $|u_\ell|_{4,K}$ can be replaced using eq (29).

$$|u_\ell|^2_{4,K} = \int_K \left(\frac{d^4 u_\ell}{dx^4}\right)^2 dx = c_1^2 \int_K \lambda_\ell^2 u_\ell^2 \, dx = c_1^2 \lambda_\ell^2 |u_\ell|^2_{0,K} \qquad (31)$$

where $c_1 = m/EI$ = constant. In (31), λ_ℓ and u_ℓ are still not available. Replacing them by their approximations leads to a computable form of the error indicator.

$$\eta_K^\ell = h_K^{2\alpha} (\lambda_\ell^h)^2 |u_\ell^h|^2_{0,K} \qquad (32)$$

We will call this type of indicator as an <u>interpolation type 2 indicator</u>.

This method has two positive features: First, it is computationally easy to implement. The L^2 norm of u_ℓ^h in (32) can be computed using multiplication of a element mass matrix and nodal value vector.

$$\int_K (u_\ell^h)^2 \, dx = \sum_i \sum_j u_i^h \left(\int_K \phi_i \phi_j dx\right) u_j^h = \sum_i \sum_j u_i^h M_{ij}^K u_j^h$$

where M_{ij}^K is the element mass matrix, u_i^h is the nodal solution vector of element K, and ϕ_i are local basis functions. We don't need to solve any system of equations as in the smoothing technique. Second, this type of the error indicator does not include higher order derivatives of u^h and, thus, seems to be more accurate. The accuracy of this indicator will also be checked in the next section. However, this method has a dificiency : It is not easy to generalize.

4.5 Accuracy of Error Indicators

In previous sections, we established error estimators for elliptic eigenvalue problems based on interpolation error estimates and proposed two types of error indicators: the interpolation type 1 and interpolation type 2.

In this section, the accuracy of error indicators is checked based on the following issues :

1. Let E_{max} denote the maximum element-wise error in the energy norm over all elements, i.e.,

$$E_{max} = \max_K E_K.$$

Let η_{max} denote the maximum error indicator over the domain, i.e.,

$$\eta_{max} = \max_K \eta_K.$$

In sec. 4.5.1, we will test the accuracy of indicators based on how accurately η_{max} estimates E_{max} This provides good guidance for improving an approximation via enrichment, i.e., determining whether an adaptive finite element scheme is needed or not.

2. Let $E_K(\%)$ denote the ratio

$$E_K(\%) = E_K / E_{max} \times 100 .$$

Let $\eta_K(\%)$ denote the ratio

$$\eta_K(\%) = \eta_K / \eta_{max} \times 100.$$

In sec. 4.5.2, we will test the accuracy of the indicators based on how accurately $\eta_K(\%)$ can estimate $E_K(\%)$ over the domain. This kind of accuracy is needed if η_K is to be used to relocate elements without enrichment.

3. Using results of sec. 4.5.1 and 4.5.2, improved grids are constructed by node relocation. Results are shown in sec.4.5.3.

Model Problem

Consider a 1-dimensional, 4th order eigenvalue problem,

$$\frac{d^4u(x)}{dx^4} = \lambda\, u(x) \qquad 0 < x < b \tag{36}$$

+ four typical types of boundary conditions

(1) pinned-pinned (SS-SS)

(2) cantilever (CL)

(3) clamped-pinned (CL-SS)

(4) clamped-clamped (CL-CL)

The ℓ-th mode eigenvalue λ_ℓ and the associated eigenfunction u_ℓ satisfy

$$\frac{d^4u_\ell(x)}{dx^4} = \lambda_\ell u_\ell(x) \qquad 0 < x < b \tag{36.a}$$

and the associated boundary conditions. The weak form associated with (36) is

$$a(u_\ell, v) = \lambda_\ell(u_\ell, v) \quad \text{for all } v \text{ in } V \tag{37}$$

$$a(u_\ell,v)= \int_0^b \frac{d^2u_\ell}{dx^2}\,\frac{d^2v}{dx^2}\,dx \qquad (u_\ell,v)= \int_0^b u_\ell v\,dx \ .$$

The associated finite element problem is as follows.

Find the approximation to the ℓ-th mode eigenpair, $(\lambda_\ell^h,u_\ell^h)$, such that

$$a(u_\ell^h,v^h) = \lambda_\ell^h(u_\ell^h,v^h) \quad \text{for all } v^h \text{ in } V^h \subset V \tag{38}$$

In this work, two types of elements are used : a <u>cubic beam element</u> and a <u>quintic beam element</u>.

Let E_K^ℓ denote the exact error in the energy norm of the ℓ-th mode eigenfunction in the element K. Then E_K^ℓ can be computed from

$$E_K^\ell = a(u_\ell-u_\ell^h,u_\ell-u_\ell^h)|_K = \int_K \left(\frac{d^2u_\ell}{dx^2} - \frac{d^2u_\ell^h}{dx^2}\right)^2 dx \ .$$

4.5.1 Accuracy on Maximum Errors

In this section, the accuracy of error indicators is tested based on how accurately they can estimate the maximum of errors.

4.5.1.1 Cubic Beam Elements

<u>Eigenvalue Error Estimates</u>

Figure 2 illustrate the relative percentage error in eigenvalues as the number of cubic beam elements (N) increases uniformly. A cubic beam element has 2 nodes and 2 dof per each node. Thus, the total number of degrees of freedom in the model is 2N (see Appendix C. for the exact eigenvalues for each case).

Eigenvalue errors decrease exponentially as N increases. Note that the Nth mode eigenvalue error of N cubic beam elements in the SS-SS case is about 22 %. From Figure 2, we can observe that the relative percentage error in the ℓ-th mode eigenvalue is the same for all modes ℓ when the numbers of elements $N = \ell, 2\ell, 3\ell$, etc are used. For example, in the SS-SS case, if the relative percentage error in the 2nd eigenvalue computed with 4 elements is 1 %, the relative percentage error in the 3rd mode computed with 6 is also 1 %. Similarly, if the relative percentage error in the 2nd eigenvalue using 6 elements is 0.1 %, the relative percentage error in the 3rd mode using 9 elements is also 0.1 %. Similar behavior of constant error can be observed in other cases. We can characterize this behavior follows: <u>The relative error in the ℓ-th mode eigenvalue is the same for all modes ℓ when the numbers of elements used in the approximation is $N = (2\ell + b), (3\ell + b)$, etc.</u> The constant b depends on the boundary conditions : b=0 in SS-SS case, b=-1 in CL case and b=1 in CL-SS and CL-CL cases. The relative percentage error of the ℓ-th mode eigenvalue is within 1 % when $N = (2\ell + b)$ is used and is between 0.1 % - 0.2 % when $N = (3\ell + b)$ is used. As will be shown next, the same behavior can also be found in the error of

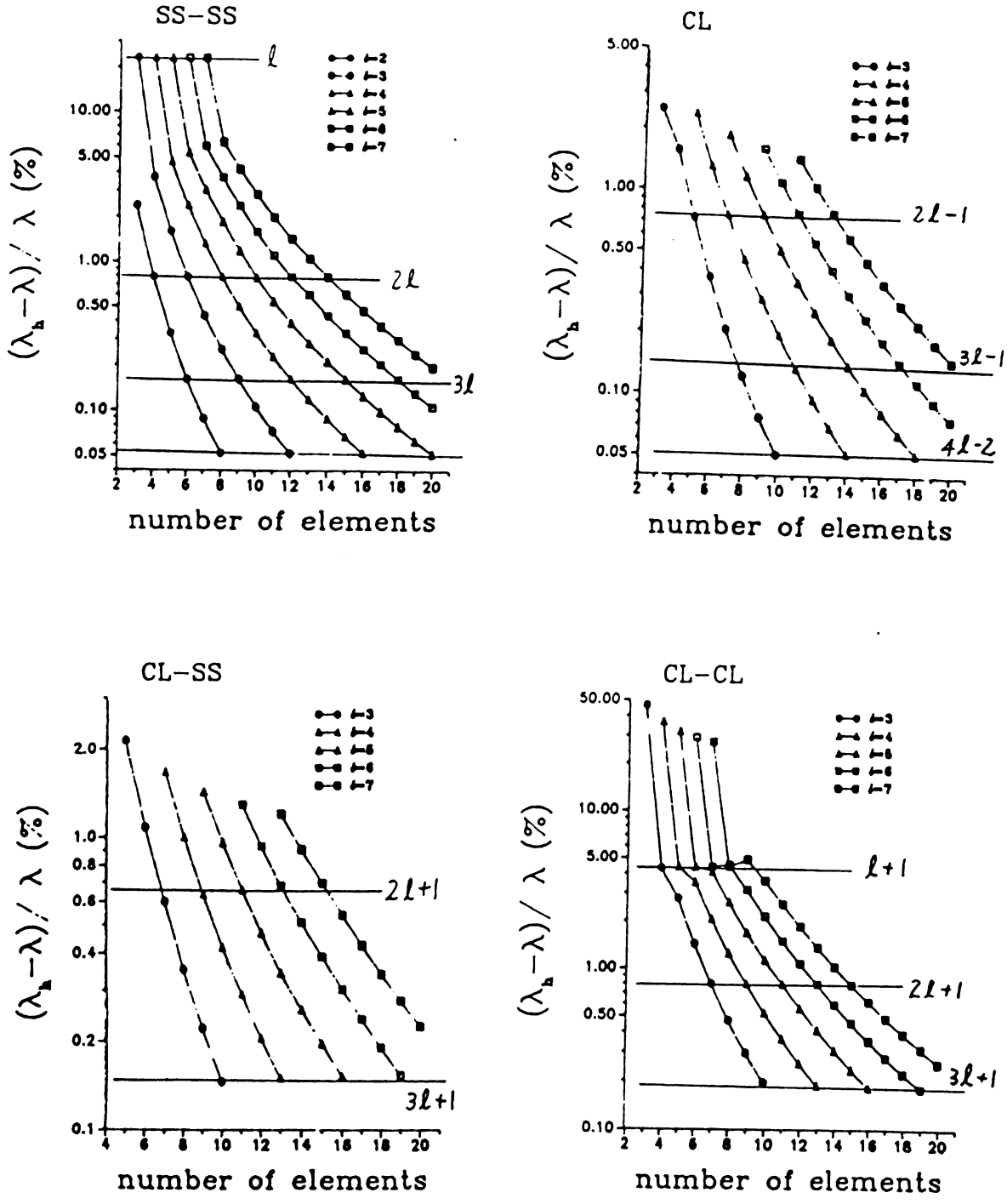

Figure 2. Relative percentage error in eigenvalues vs. Number of cubic beam elements

eigenfunctions.

Eigenfunction Error Estimates

Figure 3.1-3.4 show the results relating to errors in eigenfunctions using the energy norm, along with the associated error estimator and error indicators. Recall the form of the error estimator and indicators,

$$\epsilon_K^{\ell} = c\, h_K^{2\alpha} |u_{\ell}|^2_{k+1,K} \qquad \text{(error estimator)}$$

$$\eta_K^{\ell} = h_K^{2\alpha} |\hat{u}_{\ell}|^2_{k+1,K} \qquad \text{(error indicator)}$$

In Figure 3.1-3.4, the plots show variations in the following four kinds of values ($\max_K E_K$, $\max_K \epsilon_K$, $\max_K (\text{interp } 1)_K$, $\max_K (\text{interp } 2)_K$) for each boundary conditions as the number of cubic beam elements (N) increases.

1) $\max_K E_K$ - the maximum exact error in the energy over all elements

2) $\max_K \epsilon_K$ - the maximum error estimator over all elements

3) $\max_K (\text{interp } 1)_K$ - the maximum interpolation type 1 indicator over all elements

4) $\max_K (\text{interp } 2)_K$ - the maximum interpolation type 2 indicator over all elements

The constant c in the error estimator is assumed to be 1 and, during computation, the element length (h_K) remains unchanged, i.e., h_K is

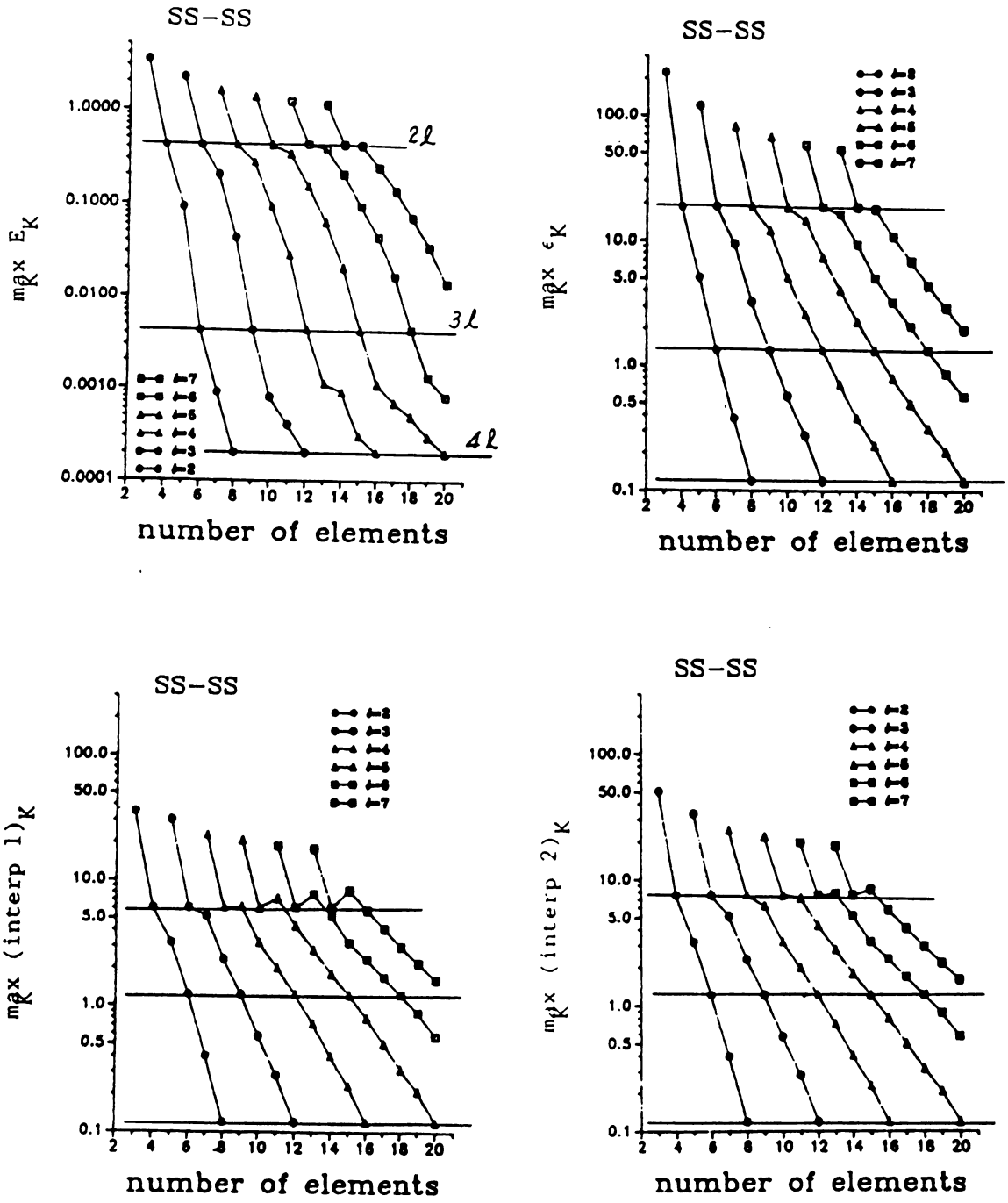

Figure 3.1 Error in eigenfunction vs. Number of cubic beam elements (pinned-pinned boundary condition)

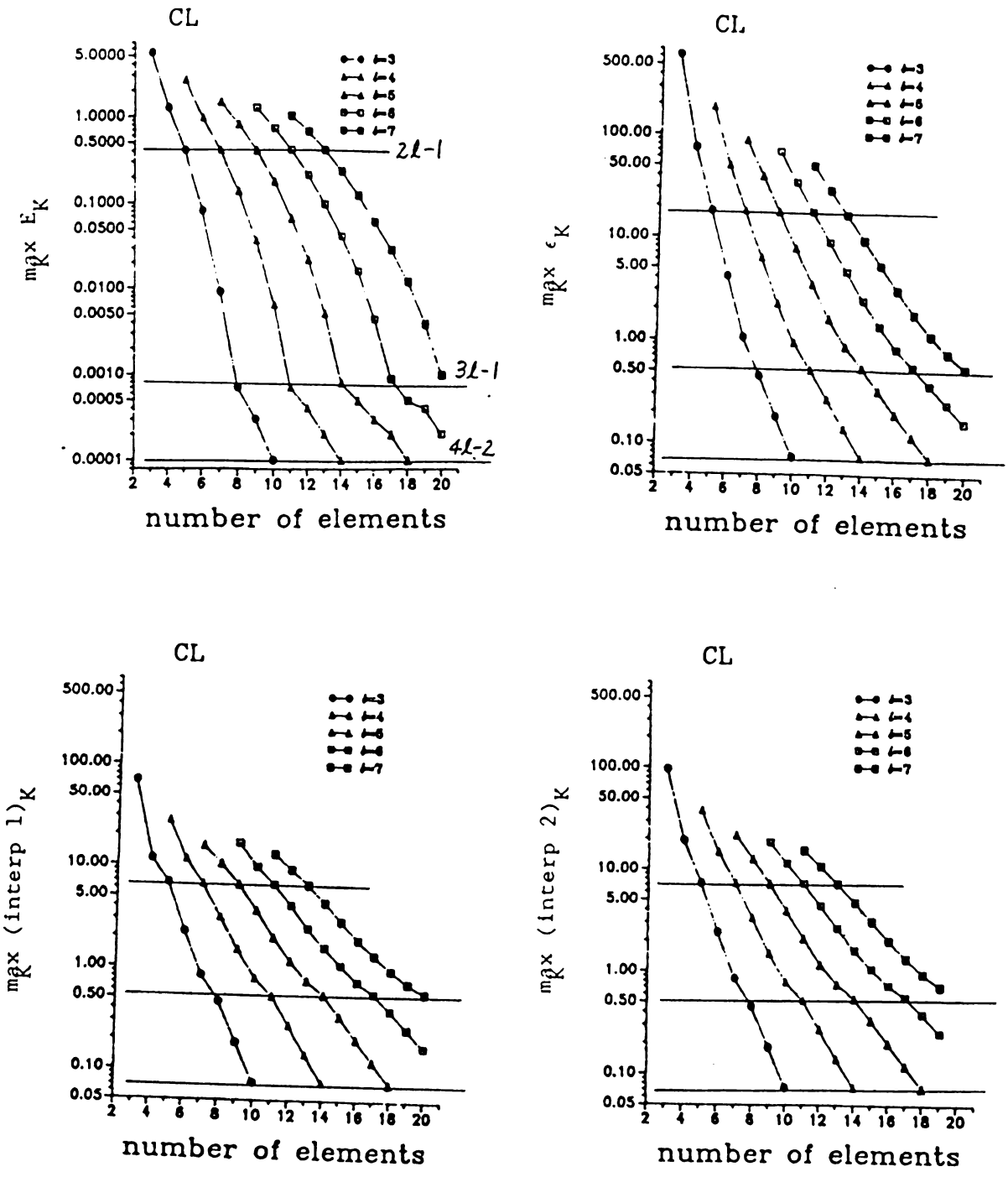

Figure 3.2 Error in eigenfunction vs. Number of cubic beam elements (clamped-free boundary condition)

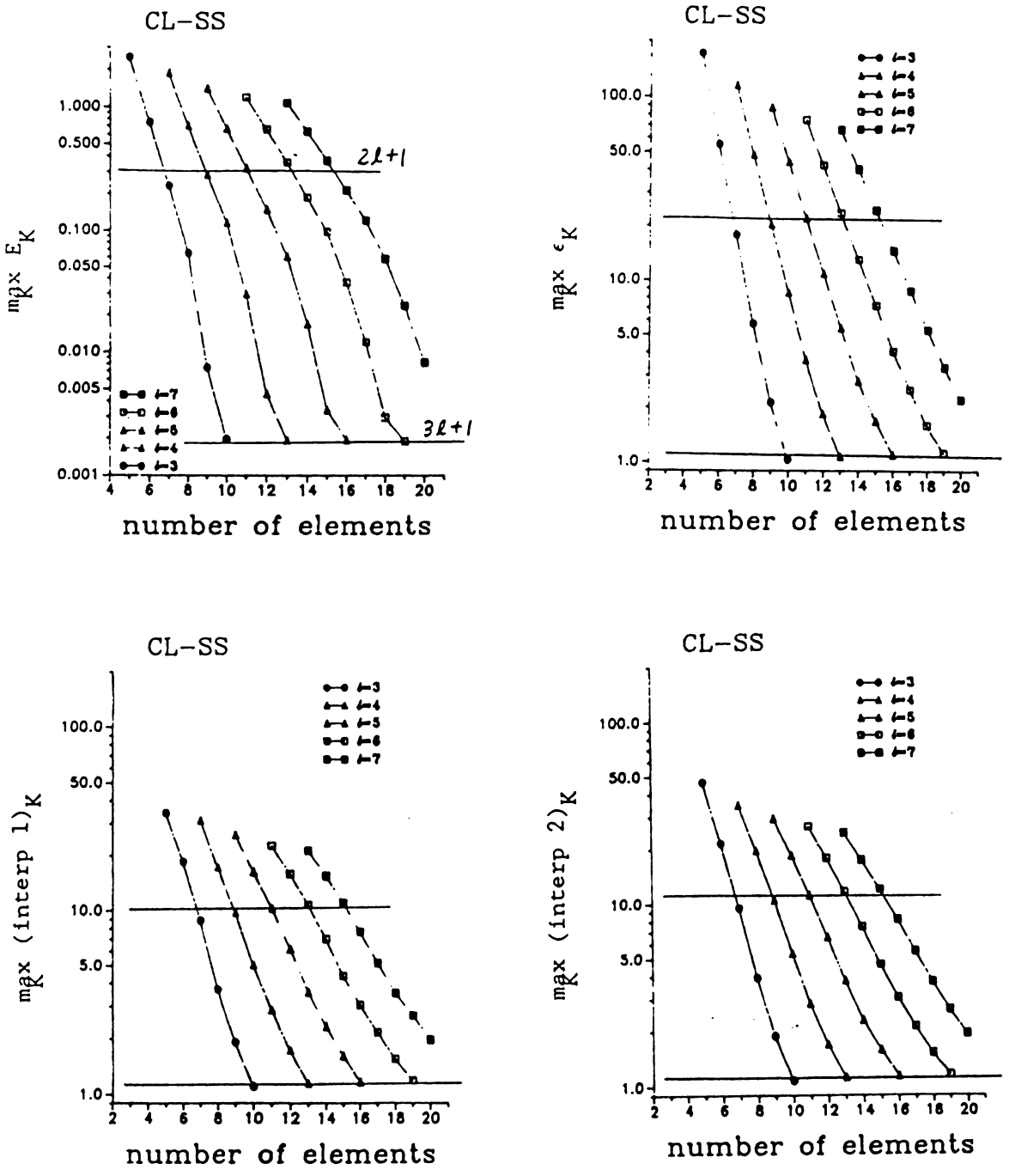

Figure 3.3 Error in eigenfunction vs. Number of cubic beam elements (clamped-pinned boundary condition)

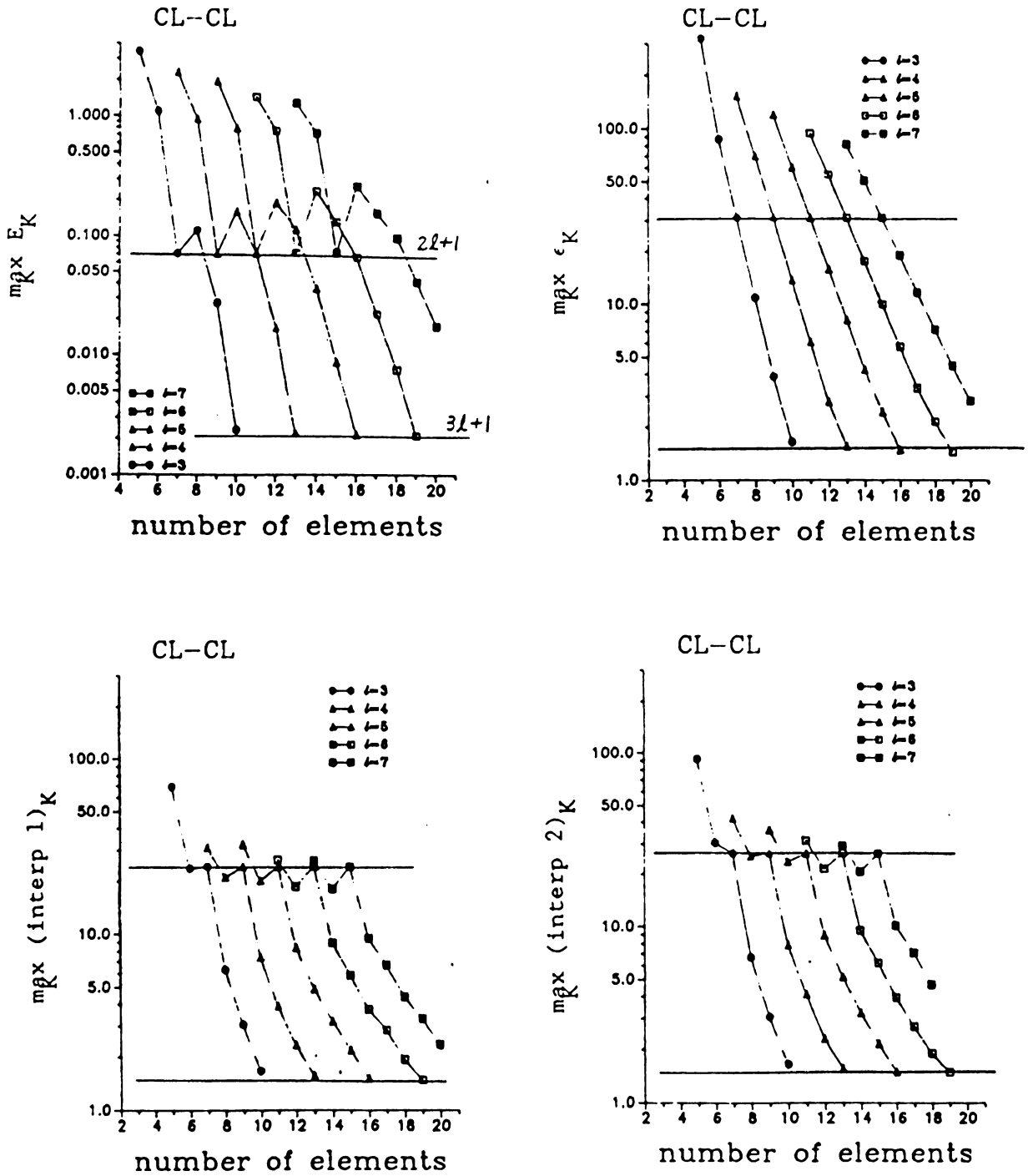

Figure 3.4 Error in eigenfunction vs. Number of cubic beam elements (clamped-clamped boundary condition)

fixed to be 1. Thus, the effect of the term $h_K^{2\alpha}$ in the error estimator and indicators is not considered in these plots (see Appendix C. for closed forms of exact eigenfunctions).

In Figure 3.1-3.4, the same behavior of constant error, found in Figure 2, is observed. The maximum error in the ℓ-th mode eigenfunction is the same for all modes ℓ when the number of elements $N = (2\ell + b), (3\ell + b)$, etc. is used. The constant b equals 0 in the SS-SS case, -1 in CL case and 1 in CL-SS and CL-CL cases. Note that this behavior can be found in all plots for the exact error in the energy norm, error estimator and error indicators.

Since the constant c in the error estimator is assumed to be 1, the accuracy of the indicators is reflected by the ratio of indicator to the estimator, i.e., $\eta_K^\ell/\epsilon_K^\ell$. Similarly, the accuracy of the maximum error indicator is reflected by $\max_K \eta_K^\ell \,/\, \max_K \epsilon_K^\ell$. Let R_1 and R_2 be such ratios, i.e.,

$$R_1 = \max_K (\text{interp } 1)_K \,/\, \max_K \epsilon_K$$

$$R_2 = \max_K (\text{interp } 2)_K \,/\, \max_K \epsilon_K \quad .$$

The indicator is said to be accurate when $R \approx 1$. From Figure 3.1-3.4, we can observe that $R_1 \approx 1$ and $R_2 \approx 1$ when $N \geq (3\ell + b)$. This means that both indicators are accurate as long as more than $(3\ell + b)$ elements are used.

4.5.1.2 Quintic Beam Elements

In the previous section, results concerning mesh refinements varying number of elements keeping the polynomial degree of basis functions fixed have been presented. In this section, we repeat the computations using a different (higher order) polynomial degree of basis functions. Quintic beam elements with 3 nodes and 2 dof/node are used (see Appendix B for the description of this type of quintic beam elements). When quintic beam elements are used, the error estimator and indicator have the form

$$\epsilon_K^{\ell} = c\, h_K^8 |u|_{6,K}^2 \quad , \quad \eta_K^{\ell} = h_K^8 |u|_{6,K}^2$$

The constant c is again assumed to be 1.

In Figure 4, the relative percentage eigenvalue error in SS-SS case is illustrated as the number of quintic beam elements (N) increases uniformly. We can observe that the eigenvalues are estimated much more accurately using quintic beam elements than using cubic beam elements.

Figure 5.1-5.4 include error estimates of eigenfunctions using quintic beam elements.

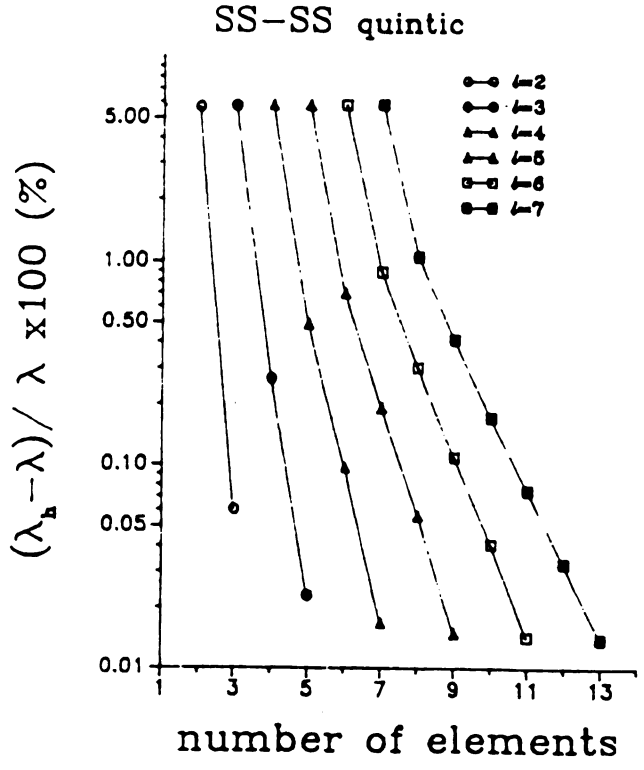

Figure 4. Relative percentage error in eigenvalue vs. Number of quintic beam elements (pinned-pinned boundary condition)

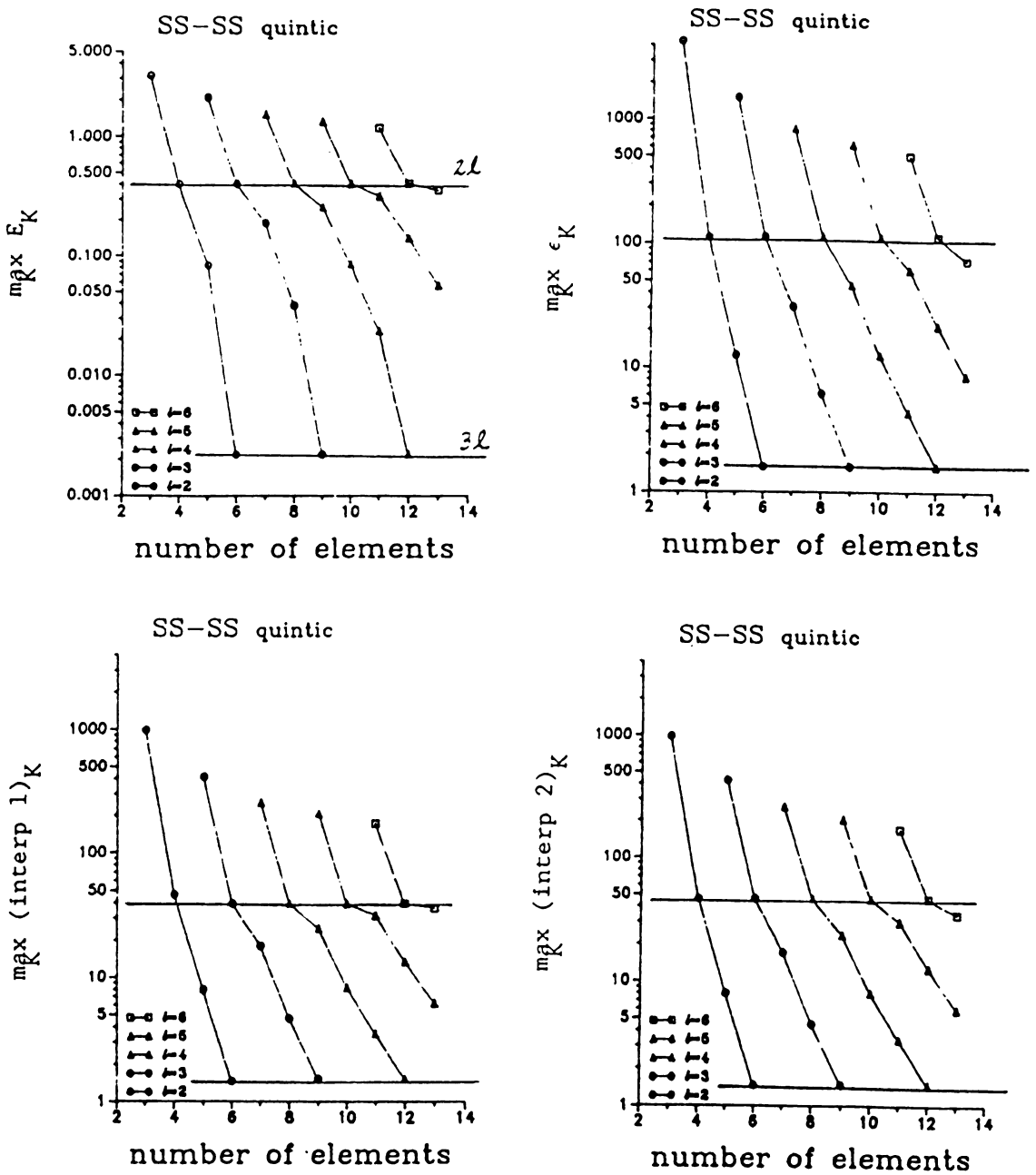

Figure 5.1 Error in eigenfunction vs. Number of quintic beam elements (pinned-pinned boundary condition)

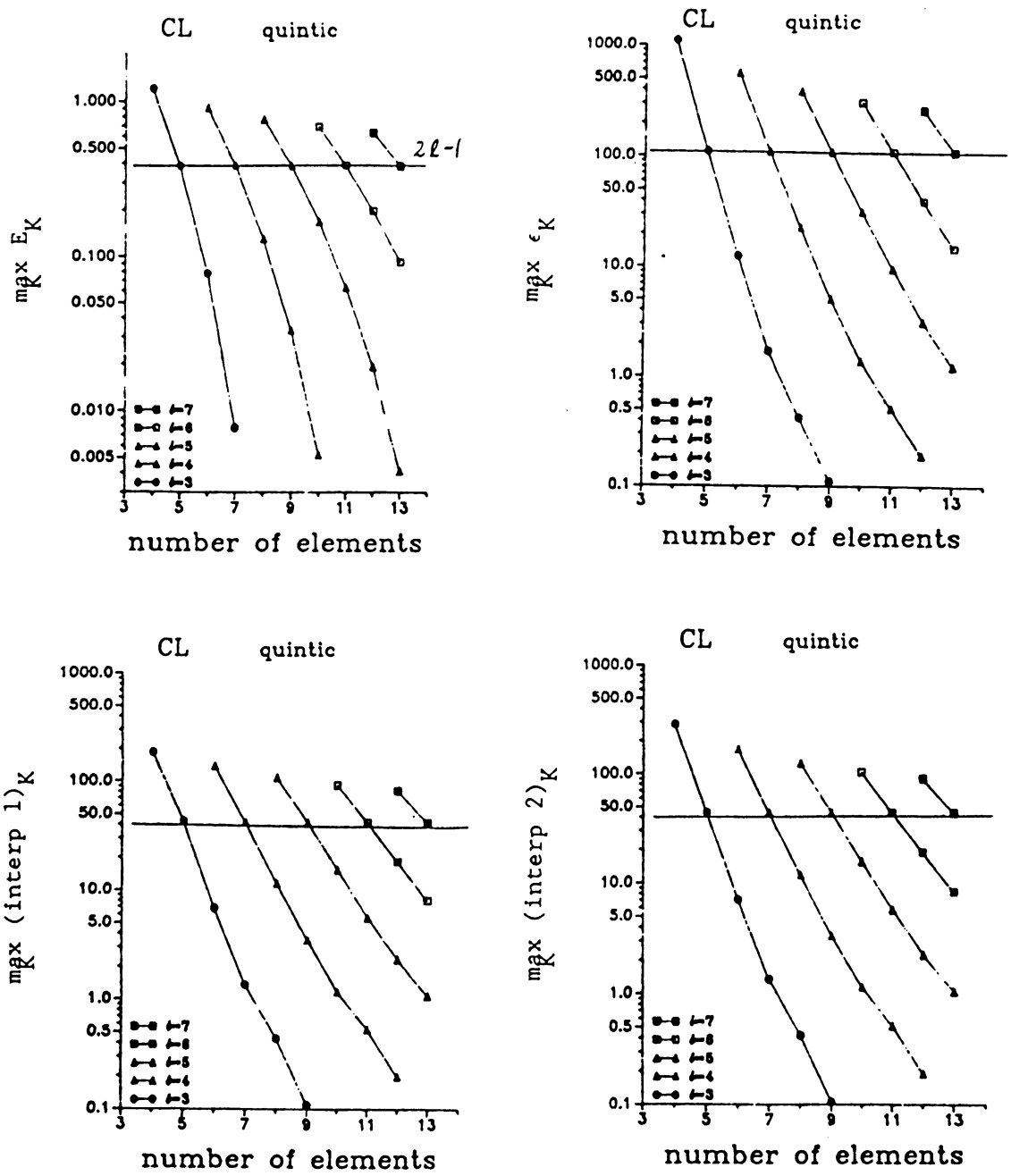

Figure 5.2 Error in eigenfunction vs. Number of quintic beam elements (clamped-free boundary condition)

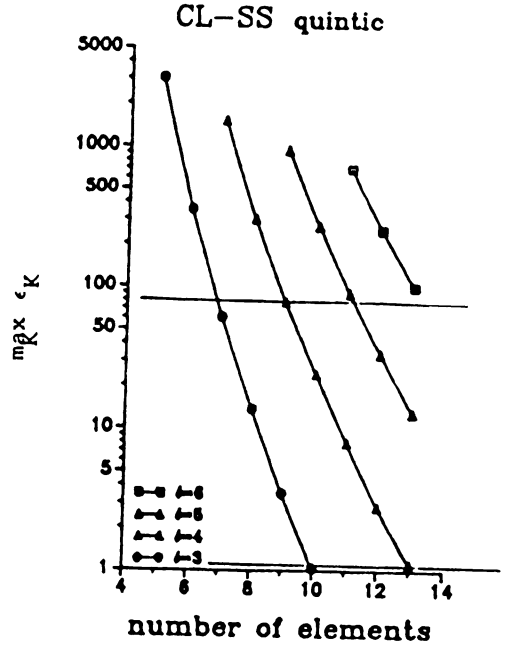

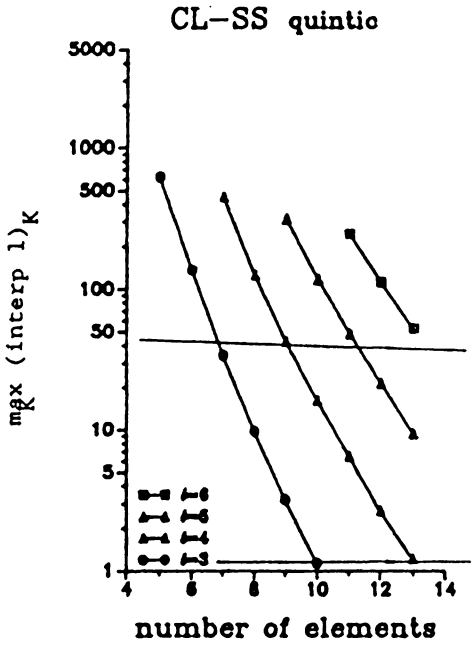

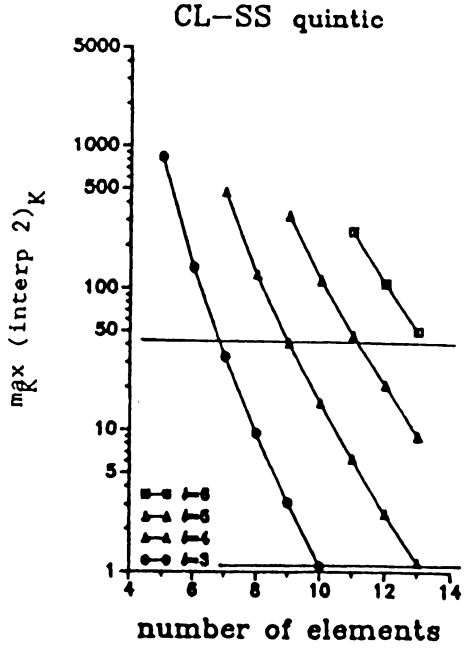

Figure 5.3 Error in eigenfunction vs. Number of quintic beam elements (clamped-pinned boundary condition)

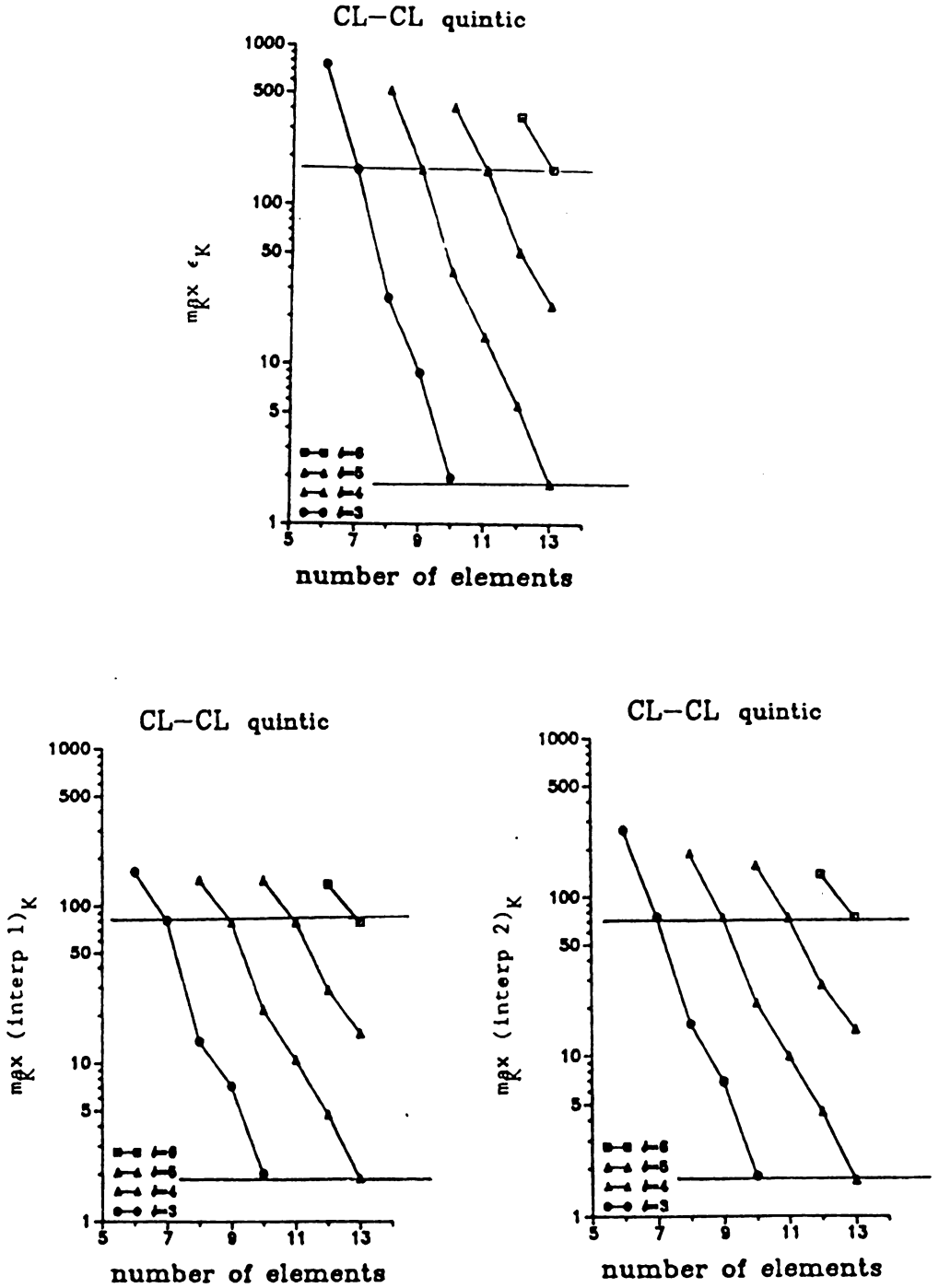

Figure 5.4 Error in eigenfunction vs. Number of quintic beam elements (clamped-clamped boundary condition)

General conclusions concerning estimates of maximum errors using indicators can be made as follows :

(1) The maximum error of the ℓ-th mode eigenfunction is the same for all modes ℓ when the number of elements $N = (2\ell + b)$, $(3\ell + b)$, etc. is used. The constant b depends on the boundary conditions. It equals 0 in SS-SS case, -1 in CL case, and 1 in CL-SS and CL-CL cases. This is true for both cubic and quintic elements and is true for the maximum error estimator and maximum error indicators.

(2) Both error indicators can estimate accurately the maximum error in the ℓ-th mode eigenfunction when more than $N= (3\ell + b)$ elements are used.

(3) Since, in general, fewer elements are preferred for practical reasons, the numbers of elements between $(2\ell + b)$ and $(3\ell + b)$ elements may be used when a certain amount of error can be accepted.

4.5.2 Accuracy on Error Distributions

In this section, the accuracy of error indicators is tested based on how accurately they can estimate the distribution of true errors over the domain. As will be discussed in the next section, the node relocation to achieve an improved grid within a fixed total degrees of freedom requires accurate estimates of the distribution of true errors over the domain.

4.5.2.1 Cubic Beam Elements

Figure 6 includes results concerning the percentage error distribution using cubic beam elements. Let $E_K(\%)$ and $\eta_K(\%)$ denote the percentage error in the energy norm and percentage error indicator corresponding to the K-th element. The percentage error distribution is computed by

$$E_K(\%) = E_K \,/\, E_{max} \times 100 \quad , \quad \eta_K(\%) = \eta_K \,/\, \eta_{max} \times 100 \ .$$

In Figure 6, three kinds of bars are shown . The height of the bar at a given location corresponds to the percentage measure ($E_K(\%)$ or $\eta_K(\%)$) at that point. In symmetric cases (SS-SS and CL-CL cases), only half of the domain is shown. The legend of three bars is descibed below.

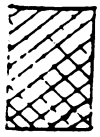

$E_K(\%) = E_K \,/\, E_{max} \times 100$

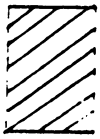

$(\text{interp } 1)_K / \max_K (\text{interp } 1)_K \times 100$

$(\text{interp } 2)_K \,/\, \max_K (\text{interp } 2)_K \times 100$

Legend for Fig. 6 and 7

The interpolation type 2 indicator can estimate the distribution of the true error more accurately than the interpolation type 1. In the SS-SS case, the interpolation type 2 indicator can estimate the distribution of the true error accurately regardless of N. However, in the CL case, $N = (3\ell + b)$ elements are needed to accurately estimate the distribution of the true error. This can be observed also in the cases, CL-SS and CL-CL. We can conclude that the interpolation type 2 indicator can estimate accurately the distribution of the true error when, in symmetric cases, more than $N = (2\ell + b)$ elements is used and, in unsymmetric cases, more than $N = (3\ell + b)$ is used.

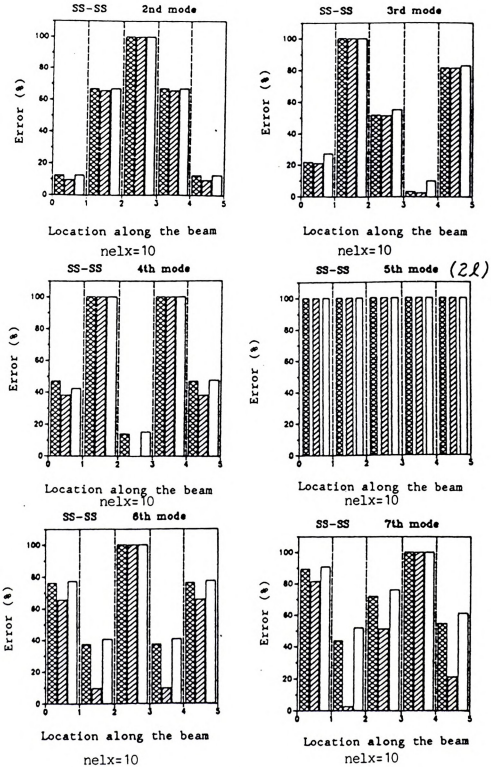

Figure 6. Percentage error vs. Location along the beam (cubic beam elements)

nelx = number of elements

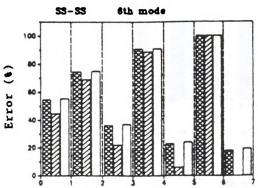

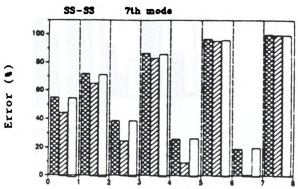

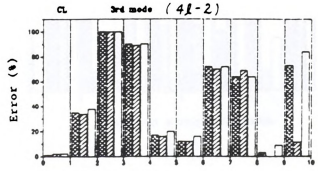

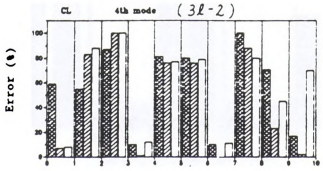

Figure 6. (cont'd)

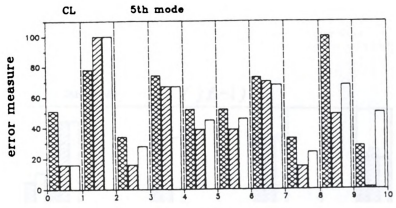

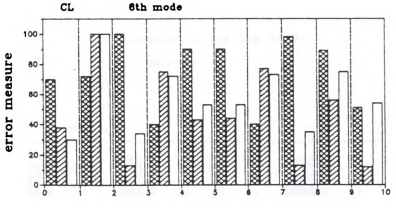

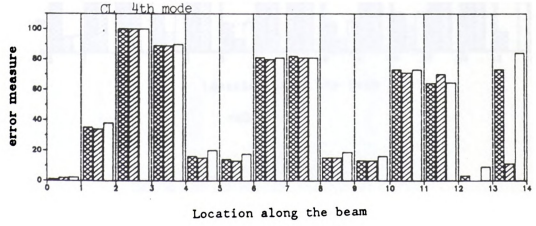

Figure 6. (cont'd)

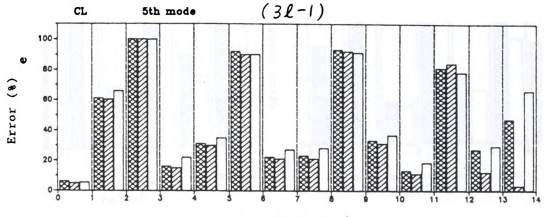

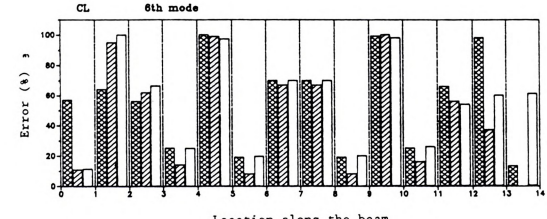

Figure 6. (cont'd)

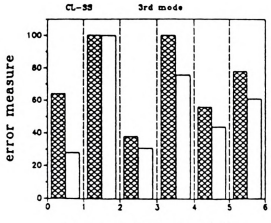

nelx=6

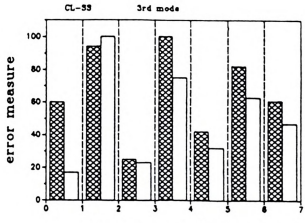

nelx=7

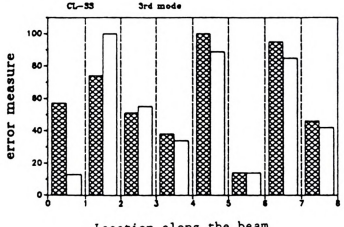

nelx=8

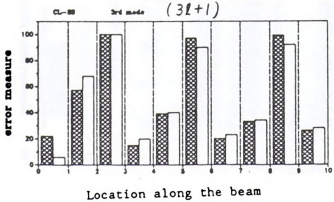

nelx=10

Figure 6. (cont'd)

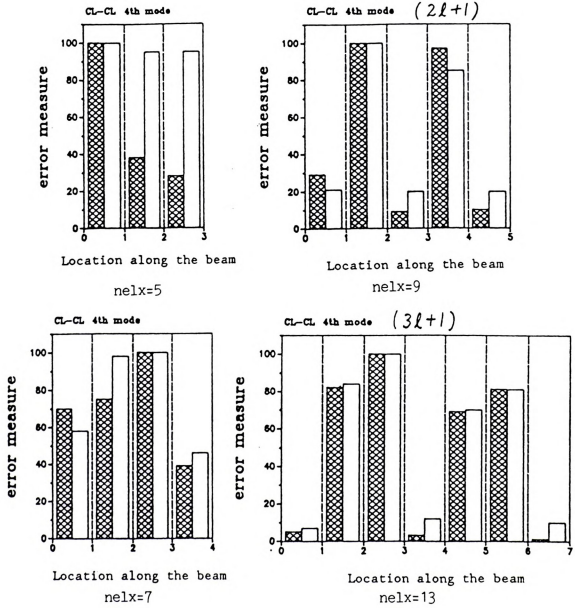

Figure 6. (cont'd)

4.5.2.2 Quintic Beam Elements

Figure 7 includes results of error distributions using quintic beam elements. Using these elements, the interpolation type 2 indicator estimates very accurately the distribution of the true error. Even in the CL case, $N = (\ell + 1)$ elements are enough to estimate accurately the error distribution for the ℓ-th mode.

Conclusions concerning the accuracy of the distribution of error indicators over the beam are as follows :

1. The interp 2 type indicator can estimate more accurately the distribution of the true error than the interpolation type 1. When higher order elements are used, the interpolation type 2 estimator can estimate error distributions very accurately.

2. Symmetric boundary conditions have an important effect on the number of elements needed to estimate accurately the error distribution. Using cubic beam elements, the interpolation 2 type indicator can estimate the distribution of the true error when $N=(2\ell \pm 1)$ elements are used in symmetric cases and $N=(3\ell \pm 1)$ elements are used in unsymmetric cases.

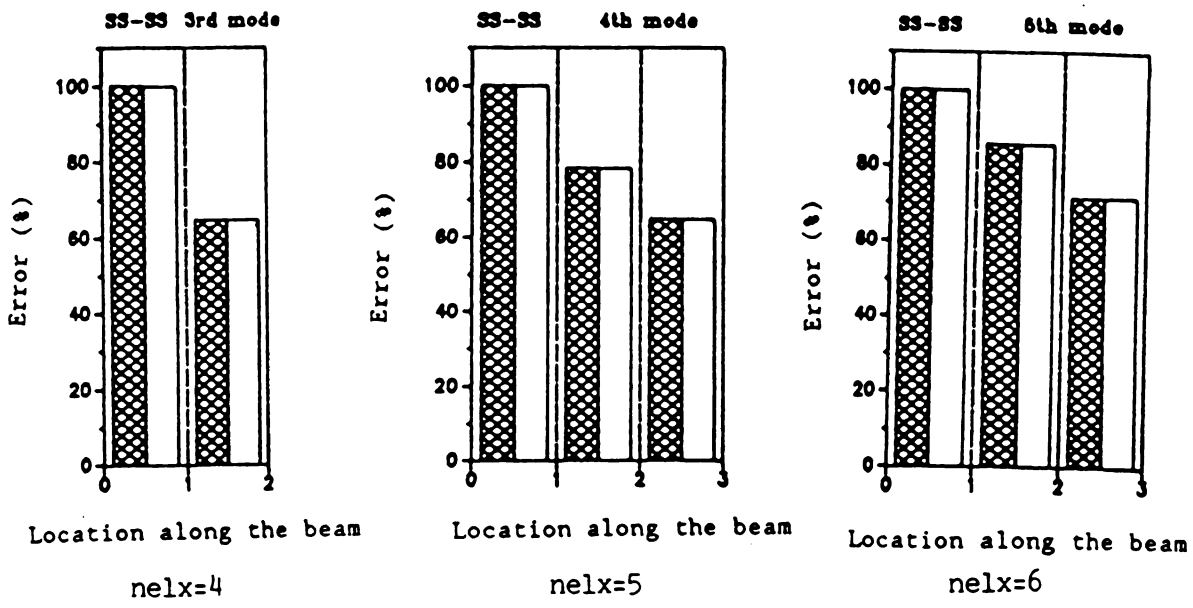

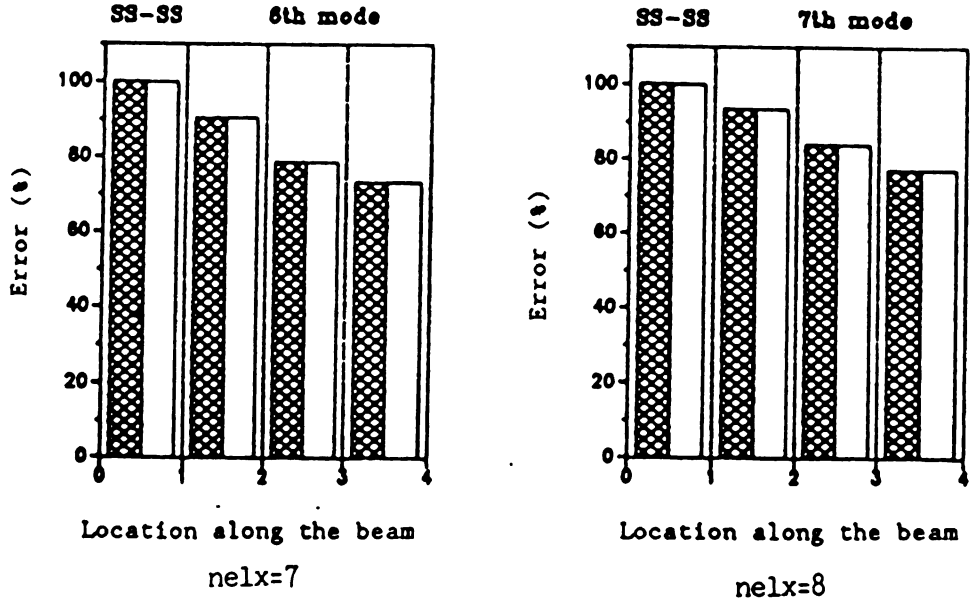

Figure 7. Percentage error vs. Location along the beam
(quintic beam elements)

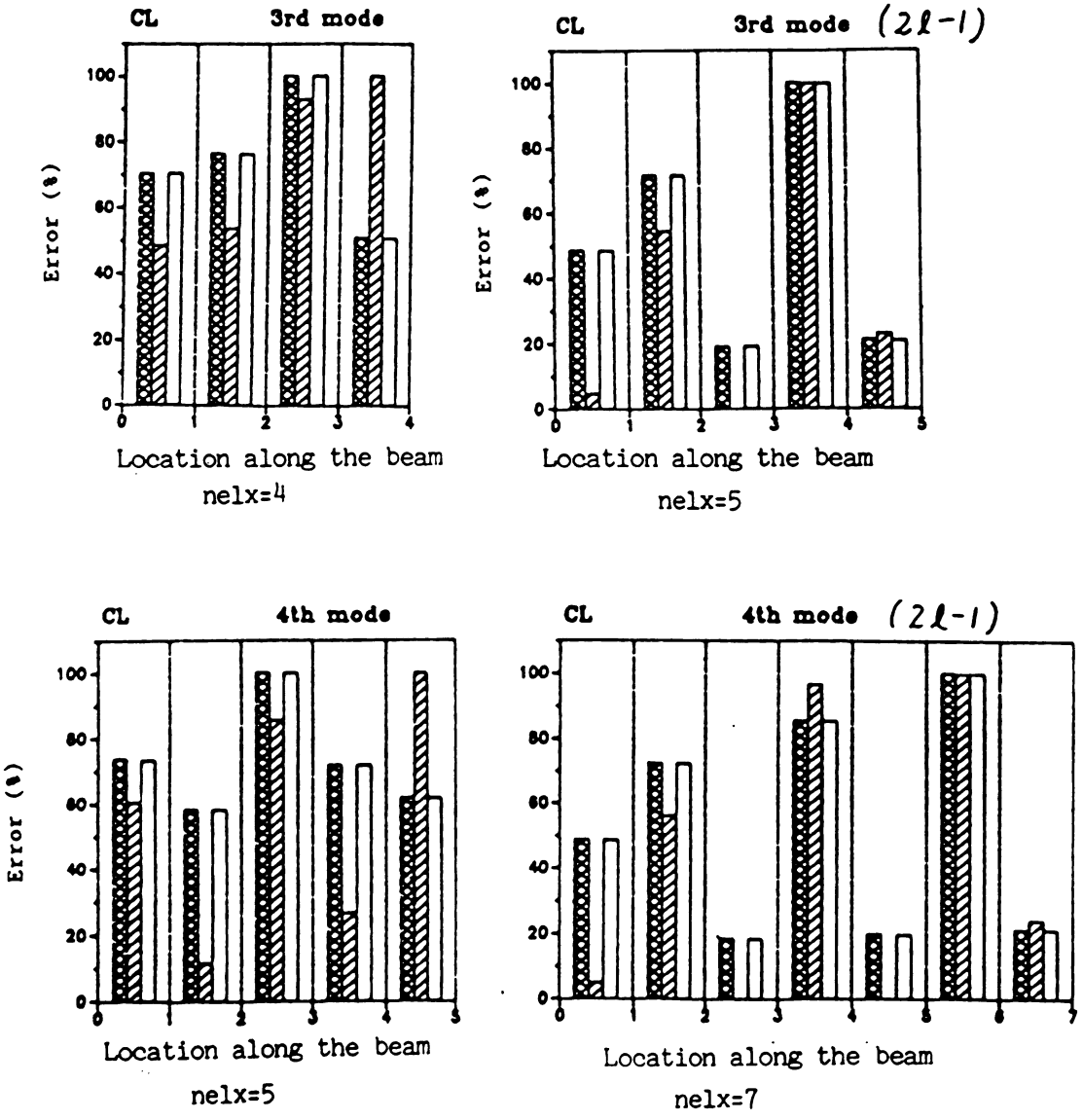

Figure 7. (cont'd)

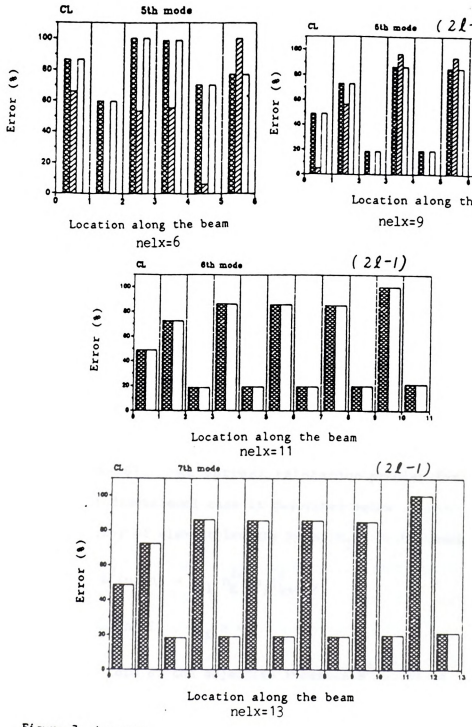

Figure 7. (cont'd)

4.5.3 Node Relocation : An Improved Grid

In this section we discuss the construction of an improved grid by node relocation within a given number of degrees of freedom. A node moving algorithm that can produce improved grids is also presented. Since it was shown that the interpolation type 2 indicator is more accurate for error distributions than the interpolation type 1 in the previous section, the interpolation type 2 indicator is used in node relocation.

In the node relocation method, the variables consist of the nodal positions as well as the nodal variables (displacements and slopes). The objective is to arrange the nodal positions so that the best possible approximation for the given total number of degrees of freedom is achieved. This has been formulated in an explicit form by Diaz et al.[14-16]. An optimal relocation problem for eigenvalue problems in a 1 dimensional case is described below.

Find the vector of element lengths $h=(h_1,h_2,\ldots,h_N)$ such that

$$\text{minimizes } B^2(u_\ell,h) = \sum_{K=1}^{N} h_K^{2\alpha} |u_\ell|^2_{k+1,K} \tag{39.a}$$

$$\text{subject to } \sum_{K=1}^{N} h_K = 1 \quad , \quad h_K \geq 0$$

The alternative form of the objective function $B^2(u_\ell,h)$ is

$$B^2(u_\ell,h) = \underset{K}{\text{Max}} \left(h_K^{2\alpha} |u_\ell|^2_{k+1,K} \right) \tag{39.b}$$

The 'true' optimality condition associated with (39.a or 39.b) is

$$f_K^{\ell} = h_K^{2\alpha} |u_{\ell}|^2_{k+1,K} = \text{constant} \quad \text{for } K=1,2,\ldots,N \tag{40}$$

Equation (40) can be used in computations using a known function $\hat{u}$ instead of u, i.e.,

$$\hat{f}_K^{\ell} = h_K^{2\alpha} |\hat{u}_{\ell}|^2_{k+1,K} = \eta_K^{\ell} = \text{constant} \quad \text{for } K=1,2,\ldots,N \tag{41}$$

where η_K^{ℓ} denotes the error indicator of the ℓ-th mode in the K-th element. Equation (41) will be referred to a 'near' optimality condition. It indicates that the near optimality condition can be achieved by relocating nodes such that error indicators are same for all elements.

To achieve the 'near' optimal (improved) grid, however, an appropriate node-moving algorithm must be proposed first. A simple node-moving algorithm was proposed by Diaz et.al. [14,15,16]. The basic idea is that a 'mass-like' quantity is assigned to each element and is assumed to be at the element's geometric center. The mass assigned to an element is proportional to the element error indicator. The mass 'attracts' the nodes surrounding it, thereby reducing the size of elements with high error. In this work, a slightly modified version is used. We assign a weighting factor to each mass such that nodes cannot move too far from their previous positions. The algorithm used in this work is presented below for a 1 dimensional case.

Let K_i denote the i-th element and X_i denote the i-th node in 1-D finite element model. The motion of the node X_i is described by

$$X_i^{new} = \frac{\eta^*_{K_{i-1}} \bar{X}_{i-1} + \eta^*_{K_i} \bar{X}_i}{\eta^*_{K_{i-1}} + \eta^*_{K_i}} \qquad \eta^*_{K_i} = \frac{(\eta_{K_i})^\beta}{L_i} \qquad (42)$$

where X_i^{new} is the new location of the node X_i, L_i is the length of element K_i, η_{K_i} is the measured error indicator of element K, $\bar{X}_i$ is the geometric center of element K and β is a weight to be assigned. If $\beta > 1$, node movements are accelerated, i.e., nodes move far from their previous positions. If $\beta < 1$, node movements are deccelerated, i.e., nodes cannot move too far from their previous positions The choice of the value of β may depend on the type of problem and thus, some preliminary tests with the different values of β may be necessary. In our problem, the weight β between 0.3 and 0.5 was proved to be a proper value. This process is repeated until the measured error indicators satisfy the near optimality condition (41) , i.e.,

$$\eta^\ell_K = \text{constant} \quad \text{for } K=1,2,\ldots,N \quad .$$

We now turn our attention to the effect of finite element nodal positions to the approximation error of eigenvalues and eigenfunctions. A simple test can illustrate this. The problem is stated as follows :

Suppose that a finite element beam model of total length l has only 2 cubic elements and 3 nodes. The first and third nodes are fixed but the second node is free to move along the beam. Our concern is the variation of the relative eigenvalue error as the second node moves along the beam and also the error in eigenfunctions in the energy norm. For this purpose, two kinds of plots are shown in Figure 8. One depicts eigenvalue errors and the other eigenfunction errors in the energy norm:

$$\text{Eigenvalue error (\%)} = \frac{(\lambda_2^h - \lambda_2)}{\lambda_2} \times 100$$

where λ_2 , λ_2^h are the 2nd mode eigenvalue and its approximation and

$$\text{Eigenfunction error (\%)} = \frac{|E_1 - E_2|}{(E_1 + E_2)} \times 100$$

where $|.|$ denotes the absolute value and E_K (K=1,2) denotes the exact error in the energy norm of the K-th element. At the optimal location, the error in elements 1 and 2 is the same, i.e., $E_1 = E_2$. At this point, the eigenfunction error (%) is 0. Vertical lines in Figure 8 denote the point where the minimum occurs.

In this test problem, symmetric cases (SS-SS and CL-CL) are special since a uniform grid of lements is actually optimal for the 2nd mode. In general, however, the optimal node location does not coincide with the uniform mesh.

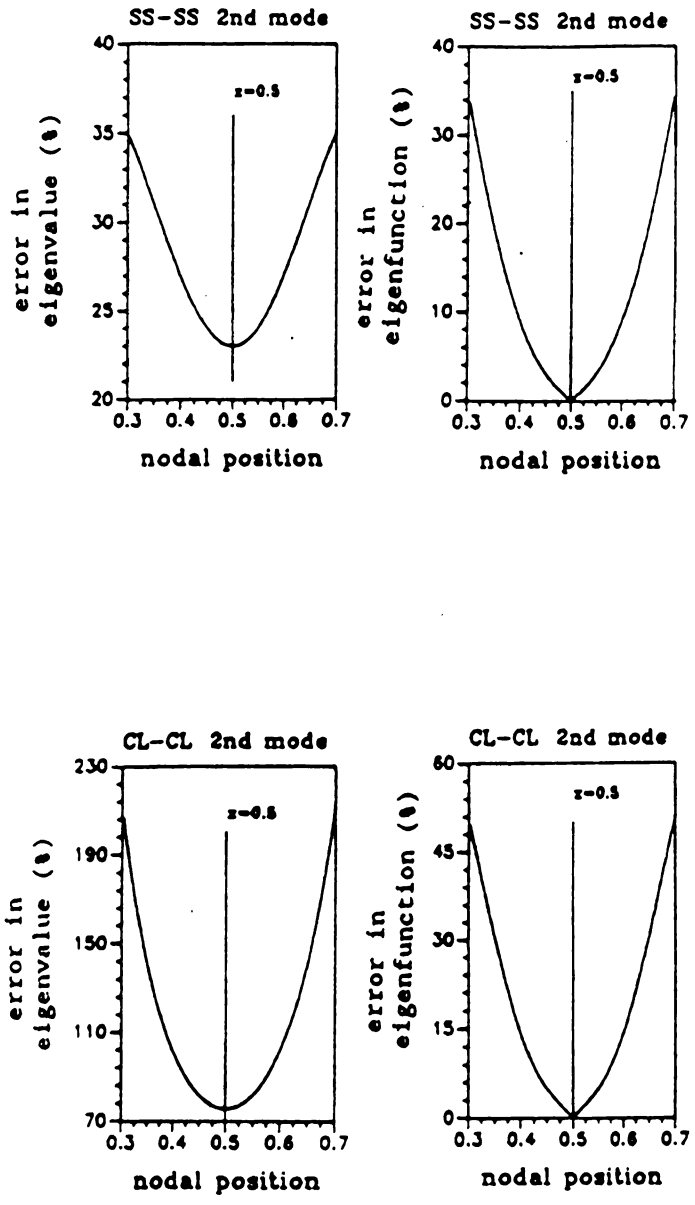

Figure 8. Error in eigenvalue and eigenfunction vs. Nodal Position

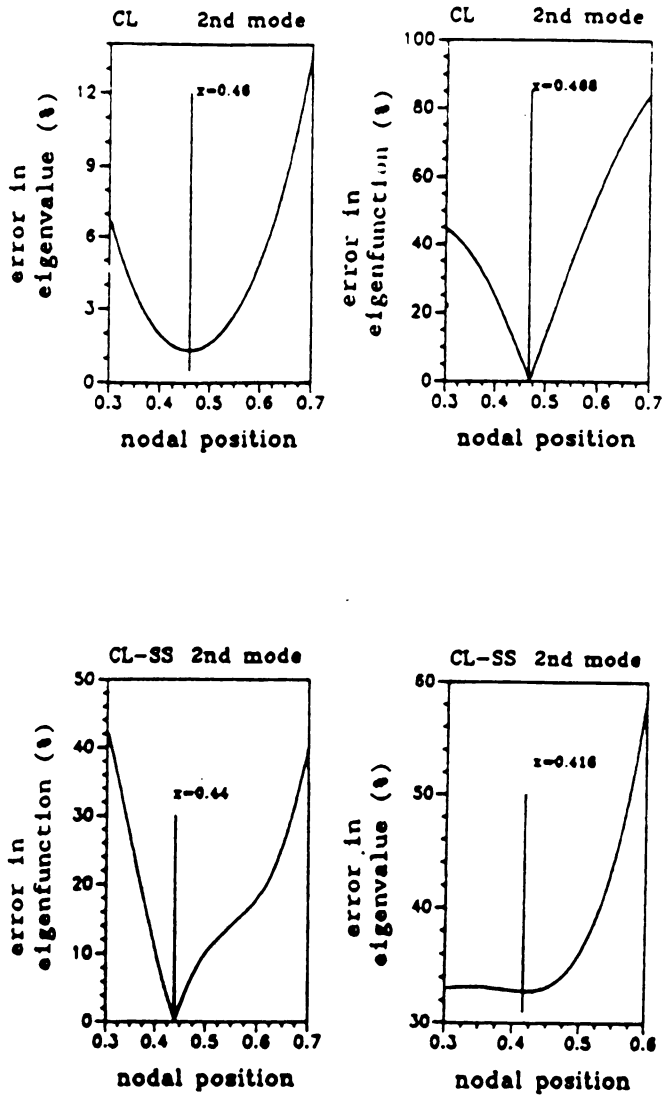
CL 2nd mode
error in eigenvalue (%)
x=0.46
nodal position
CL 2nd mode
error in eigenfunction (%)
x=0.466
nodal position
CL-SS 2nd mode
error in eigenfunction (%)
x=0.44
nodal position
CL-SS 2nd mode
error in eigenvalue (%)
x=0.416
nodal position

Fig. 8. (cont'd)

Other results related to node relocation are illustrated in Figure 9, where numerical results associated with the improved grid with respect to a single mode are presented. There, two kinds of plots are shown. One depicts the error distribution of the uniform and improved grid based only on the interpolation type 2 indicator. The other depicts the error distribution of the exact error in the energy norm using the same grids. The dotted line is the error distribution of the uniform grid and the solid line the error distribution of the improved grid. A 10 element mesh is used in all cases except in the CL-CL case, where only 7 elements are used. In symmetric cases (SS-SS and CL-CL cases), modes up to 4th are tested. In unsymmetric cases (CL and CL-SS cases), modes up to 3rd are tested.

In Figure 10, the nodal location of the improved grids anf improved eigenvalue with respect to a single mode is illustrated in two cases, SS-SS and CL cases. Table 1 lists eigenvalues and relative errors for the uniform grid in those cases.

Symmetric cases (SS-SS and CL-CL cases) need $N = (2\ell + b)$ elements for accurate estimates of error distributions, whereas unsymmetric cases (CL and CL-SS cases) need $N = (3\ell + b)$ elements.

In all cases except the 4th mode in SS-SS case, the similar reductions in both the exact error and in the indicator can be achieved. For example, suppose that after node relocations the maximum indicator is reduced by 50 %. Then we can expect that the maximum exact error will be also reduced by about 50 %.

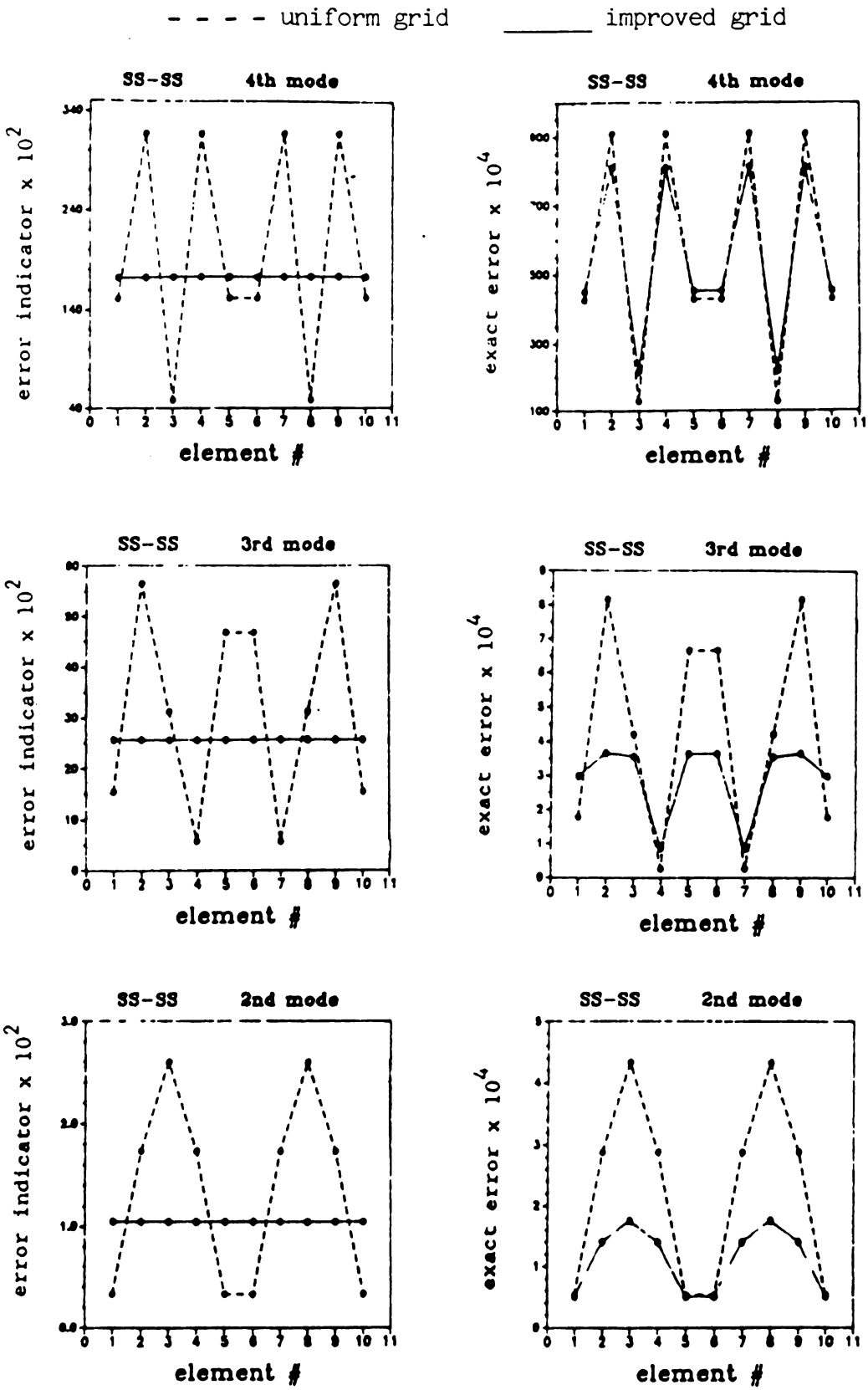

Figure 9. Error distribution of uniform and improved grid

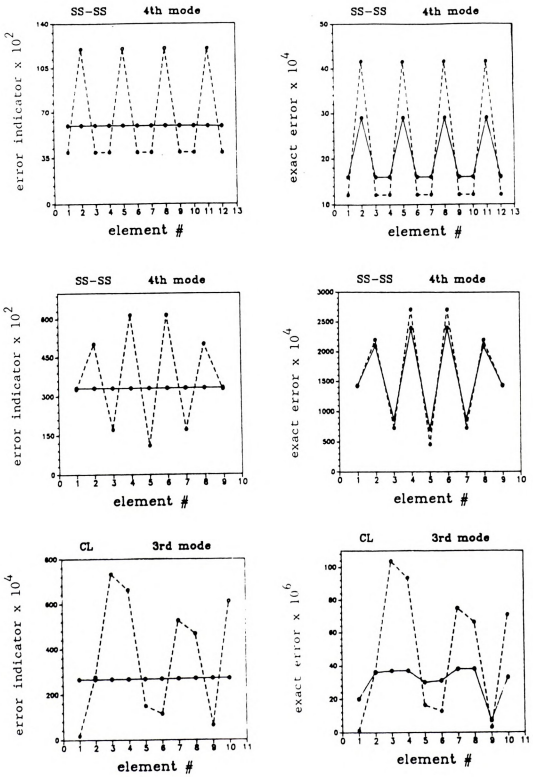

Figure 9. (cont'd)

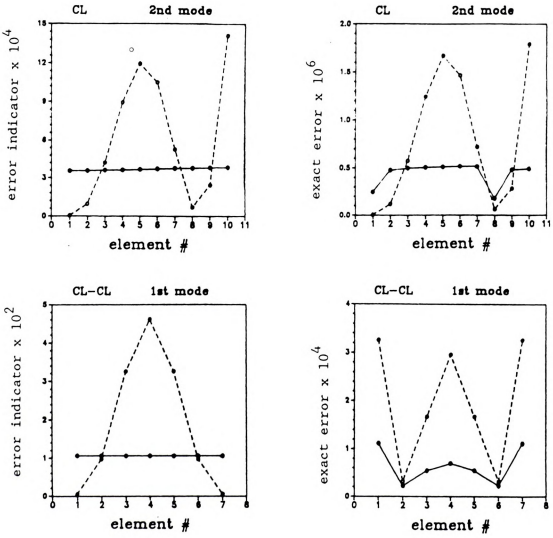

Figure 9. (cont'd)

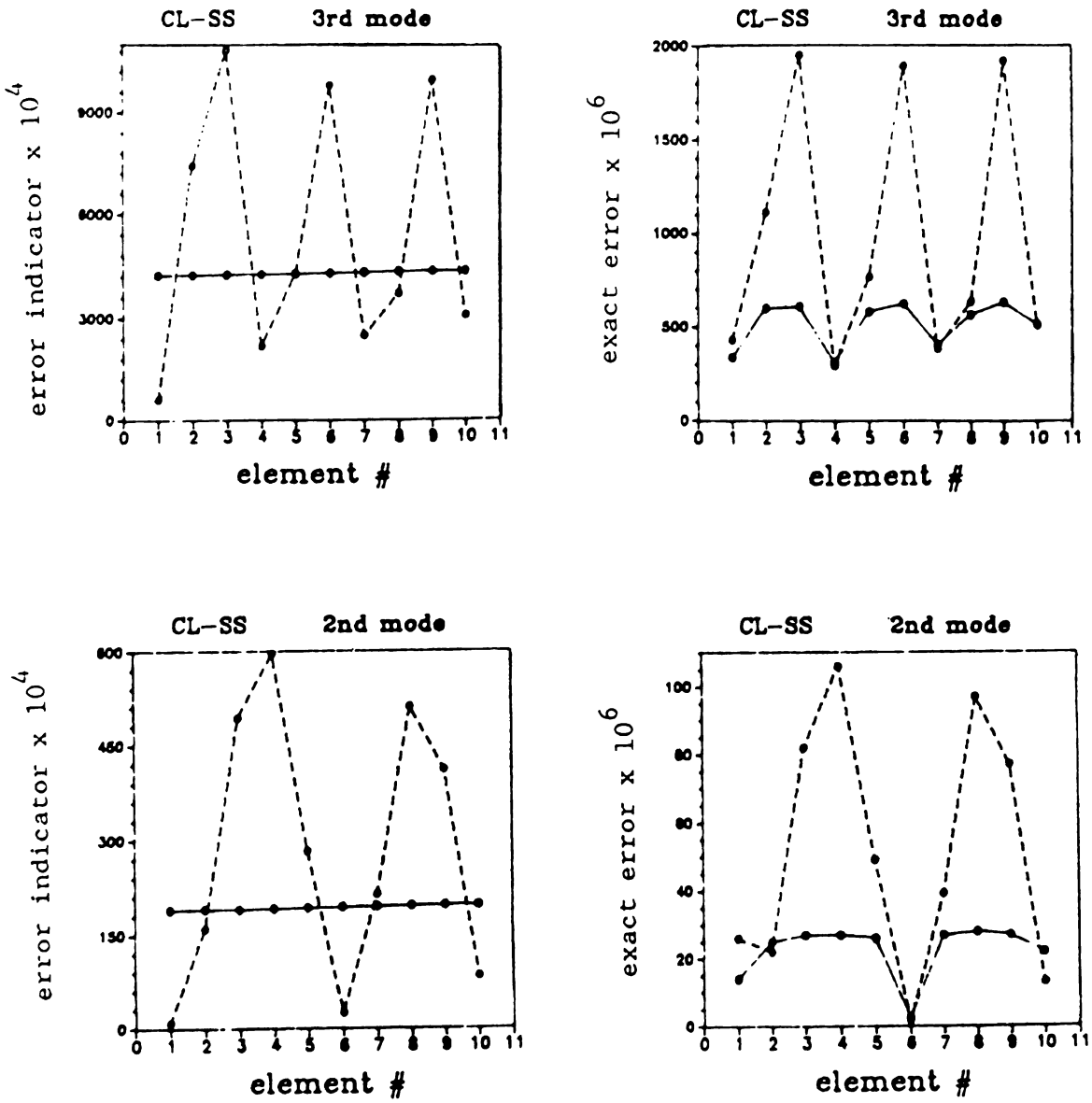

Figure 9. (cont'd)

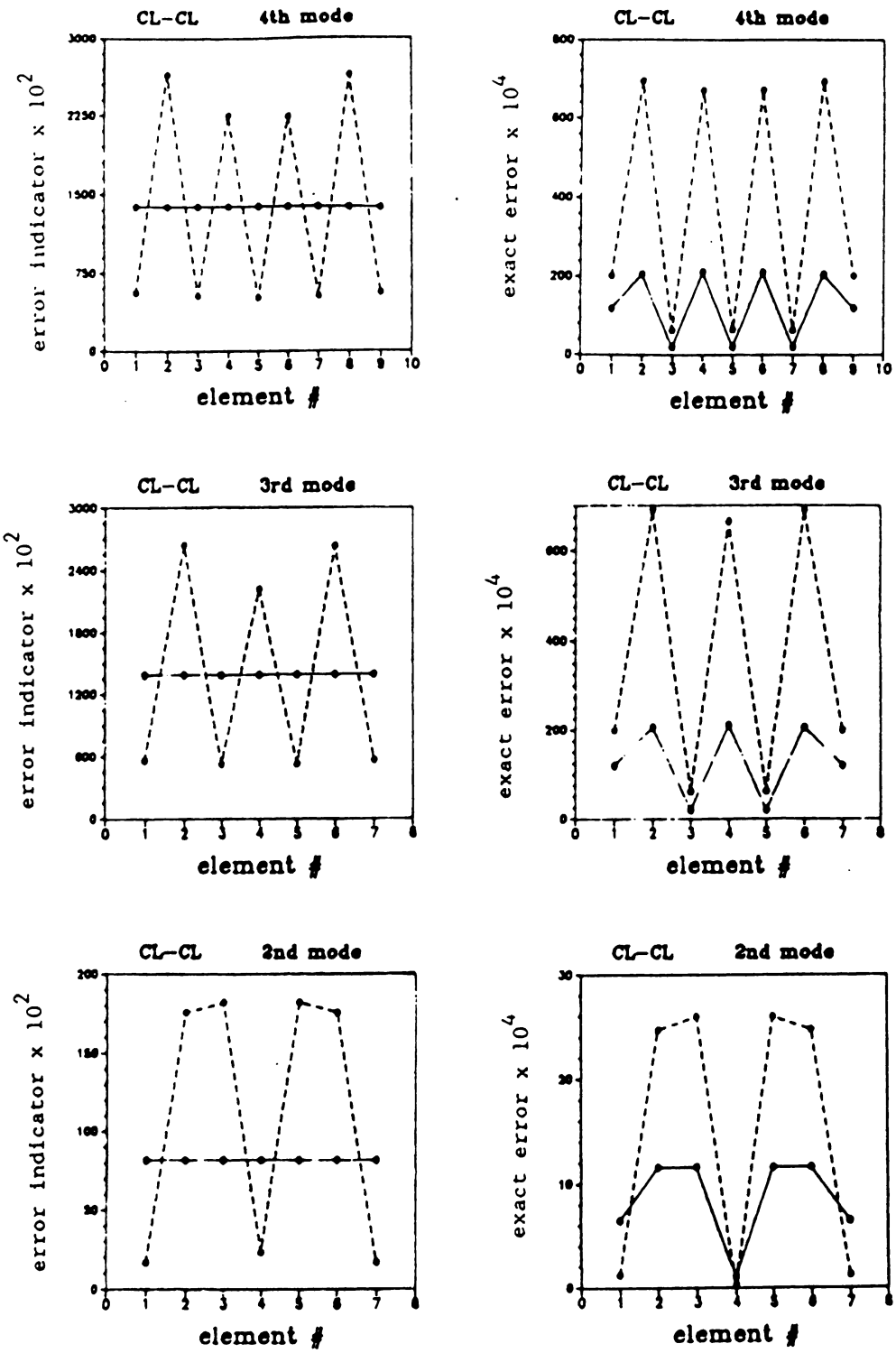

Figure 9. (cont'd)

pined-pined (SS-SS)

uniform grid

2nd mode optimized grid

λ_2 = 1558.79439

3rd mode optimized grid

λ_3 = 7895.98101

4th mode optimized grid

λ_4 = 24996.22791

cantilever (CL)

uniform grid

2nd mode optimized grid

λ_2 = 485.53422

3rd mode optimized grid

λ_3 = 3807.76813

Figure 10. Nodal location of the improved grid

PINED-PINED (SS-SS) CASE	MODE	EIGENVALUE	REL ERROR(%)
NUMBER OF ELEMENTS - 10	2	1558.87662	0.0212481848
	3	7898.54283	0.1065438590
	4	25019.26421	0.3309853171
CANTILEVER (CL) CASE	MODE	EIGENVALUE	REL ERROR(%)
NUMBER OF ELEMENTS- 10	2	485.54857	0.0061282991
	3	3808.46023	0.0502809047
CLAMPED-PINED (CL-SS) CASE	MODE	EIGENVALUE	REL ERROR(%)
NUMBER OF ELEMENTS- 10	1	237.72772	0.0027999471
	2	2497.32518	0.0335568255
	3	10883.44947	0.1460053260
CLAPMED-CLAMPED (CL-CL) CASE	MODE	EIGENVALUE	REL ERROR(%)
NUMBER OF ELEMENTS- 7	1	500.69958	0.0271058632
	2	3811.58909	0.2116979730
	3	14733.62586	0.7935330701

Table 1. Eigenvalues and relative errors for the uniform grid

CHAPTER V.

CONCLUSIONS AND RECOMMENDATIONS

5.1 Conclusions

We established error estimates for elliptic eigenvalue problems for each mode based on interpolation error theory. The error indicator was implemented using two different techniques, the smoothing technique and the direct substitution technique. The accuracy of error indicators was checked using the eigenvalue problem of a uniform, Bernoulli-Euler beam.

Based on the accuracy on maximum error, the following conclusions were drawn :

(1) The maximum error of the ℓ-th mode eigenfunction is the same for all modes ℓ when the number of elements $N = (2\ell + b)$, $(3\ell + b)$, etc. is used. The constant b depends on the boundary conditions. It equals 0 in the SS-SS case, -1 in the CL case, and 1 in the CL-SS and the CL-CL cases. This is true for both cubic and quintic elements and is true for the maximum error estimator and maximum error indicators.

(2) Both error indicators can estimate accurately the maximum

error in the ℓ-th mode eigenfunction when more than N= (3ℓ + b) elements are used.

Based on the accuracy on error distributions, the following conclusions were drawn:

(1) The interp type 2 indicator can estimate more accurately the distribution of the true error than the interpolation type 1. When higher order elements are used, the interpolation type 2 estimator can estimate error distributions very accurately.

(2) Symmetric boundary conditions have an important effect on the number of elements needed to estimate accurately the error distribution. Using cubic beam elements, the interpolation type 2 indicator can estimate accurately the distribution of the true error when N=($2\ell \pm 1$) elements are used in symmetric cases and N=($3\ell \pm 1$) elements are used in unsymmetric cases.

Using these results, improved grids were constructed by node relocation. It was observed that the similar reductions in both the exact error and in the indicator were achieved.

5.2 Discussions and Future Reasearch

The results from the improved grids (e.g. improved eigenvalues and eigenfunctions) may not be so impressive. The reason is that, in our model problem (eigenvalue problem of the uniform, Bernoulli-Euler

beam), the uniform grid itself can estimate lower mode eigenvalues with enough accuracy. An extension of 1-D beam problems to 2-D, 4th order problems (e.g. vibration of plates) may be another candidate. Main issues in 2-D problems are somewhat different from those in 1-D problems. In 1-D problems, the issue is 'how many elements' and 'what type of element' are needed to estimate eigenfunctions with enough accuracy. In 2-D problems, however, an important issue is 'where we should put additional elements'.

Accuracy estimates of eigenvalue problems may be applied to many engineering problems. As a familiar example of a stability problem from solid mechanics, the buckling of a column may be one candidate. Here, the buckling load is proportional to the smallest eigenvalue for the corresponding differential operator of beam theory and buckling mode is the associated eigenfunction.

Accuracy estimates for 1-D finite element eigenvalue problems may also be applied to modelling of beam-like structures for control design problems. In the development of feedback control theory for distributed parameter systems (DPS) which are described by partial differential equations, it is important to design an implementable finite dimensional controller. The implementation is usually done with on-line digital computers. The dimension of the controller is directly related to the memory capacity and the access time for retrieval of information from the computer memory. Therefore, the controller of the least possible dimension is preferred from a practical point of view. In order to design the finite dimensional

controller often a reduced order model (ROM) is sought. If the actual modes (eigenfuntions) are known, the dimension of the DPS may be reduced using projection into a modal space. In general, however, these modes are never known exactly and some other reasonable approximation procedure must be used. One popular choice is the finite element method [35,36]. The feedback control force or moment is computed based on approximated mode shapes and mode slopes, and is applied to atabilize the motion of the DPS. The accuracy of approximated solutions affect the stabilty of the DPS. To design the proper ROM, following two issues may be resolved :

1. Model selection problem, i.e., 'how many' and 'which' modes should be retained in the ROM. A modal cost analysis [38,39] may resolve this issue.

2. Finite element modeling problem, i.e., 'what type' and 'how many' elements should be used in the finite element ROM to produce stability of the original DPS. Accuracy estimates may resolve this.

LIST OF REFERENCES

[1] **Babuska, I. and Rheinbolt, W.C.**,"Adaptive Approaches and Reliability Estimations in Finite Element Analysis" Comp. Meth. Appl. Mech. Engrg. (1979) pp 519-540

[2] _____,"A Posteriori Error Estimates for the Finite Element Method" Int. J. Num. Meth. Engrg. 12 (1978) pp 1597-1615

[3] _____,"Error Estimates for Adaptive Finite Element Computations" SIAM J. Numer. Anal. 15(4) (1978) pp 736-754

[4] _____,"Reliable Error Estimation and Mesh Adaptation for the Finite Element Method" in Oden, J.T. ed., Computational Methods in Nonlinear Mechanics pp 67-108 North-Holland Publishing Company (1980)

[5] **Demkowicz, L.,Delvoo, Ph. and Oden, J.T.**,"On an h-type Mesh-Refinement Strategy Based on Minimization of Interpolation Errors" Comp. Meth. Appl. Mech. Engrg. 53 (1985) pp 67-89

[6] **Babuska, I. and Miller, A.**,"The Post-Processing Approach in the Finite Element Method" Part I: Calculation of Displacements, Stresses and Other Higher Derivatives of the Displacements Part II: The Calculation of Stress Intensity Factor Int. J. Num. Meth. Engrg. 20 (1984) pp 1085-1121

[7] **Babuska, I.,Szabo, B.A. and Katz, I.N.**,"The p-version of the FEM" SIAM J. Numer. Anal. 18 (1981) pp 515-545

[8] **Zienkiewicz, O.C.,Gago, J. and Kelly, D.W.**,"The Hierarchical Concept in Finite Element Analysis" Computers and Structures 16 (1983) pp 53-65

[9] **Zienkiewicz, O.C.,Kelly, D.W.,Gago, J. and Babuska,I.**, "Hierarchical Finite Element Approaches, Adaptive Refinement and Error Estimates" Proc. MAFELAP 1981

[10] **Zienkiewicz, O.C. and Craig, A.**, "Adaptive Refinement, Error Estimates, Multigrid Solution, and Hierarchic Finite Element Method Concepts " in Accuracy Estimates and Adaptive Refinements in Finite Element Computations (1986), John Wiley & Sons Ltd.

[11] **Szabo, B.A.**, "Estimation and Control of Error Based on p-convergence" in Accuracy Estimates and Adaptive Refinements in Finite Element Computations (1986), John Wiley & Sons Ltd.

[12] **Babuska, I. and Szabo, B.**,"On the Rate of Convergence of FEM" Int. J. Num. Meth. Engrg. 18 (1982) pp 323-341

[13] **Babuska, I. and Dorr, M.R.** ,"Error Estimates for the Combined h and p Versions of the FEM" Numer. Math. 37 (1981) pp 257-277

[14] **Diaz, A.R.,Kikuchi, N. and Taylor, J.E.**,"A Method of Grid Optimization for FE Methods" Comp. Meth. Appl. Mech. Engrg. 41 (1983) pp 29-45

[15] _____,"Optimal Design Formulations for Finite Element Grid Adaptation" in Komkov V. eds, Sensitivity of Functionals with Application to Engineering Science, Lecture Notes in Mathematics 1086 pp 56-76

[16] **Diaz, A.R.,Kikuchi, N.,Papalambros, P. and Taylor, J.E.**,"Design of an Optimal Grid for FE Methods" J. Struct. Mech. 11(2) (1983) pp 215-230

[17] **Kikuchi, N.**,"Adaptive Grid Design Methods for FE Analysis" Comp. Meth. Appl. Mech. Engrg. 55 (1986) pp 129-160

[18] **Demkowicz, L. and Oden, J.T.** ,"On a Mesh Optimization Method based on a Minimization of Interpolation Error" Int. J. Engrg. Sci. 24(1) (1986) pp 55-68

[19] **Shephard, M.S.,Yerry, M.A. and Bachmann, P.L.**,"Automatic Mesh Generation Allowing for Efficient a prior and a posteriori Mesh Refinement" Comp. Meth. Appl. Mech. Engrg. 55 (1986) pp 161-180

[20] **Bennighof, J.K. and Meirovitch, L.**,"Eigenvalue Convergence in the Finite Element Method" Int. J. Num. Meth. in Engrg. 23 (1986) pp 2153-2165

[21] **Friberg, P.O.**,"An Error Indicator for the Generalized Eigenvalue Problem using Hierarchical FEM" Int. J. Num. Meth. in Engrg. 23 (1986) pp 91-98

[22] **Friberg, P.O. and Moller, P. Makovicka, D. and Wieberg, N.E.**, "An Adaptive Procedure for Eigenvalue Problems using Hierarchical FEM" 24 (1987) pp 319-335

[23] **Miller, K. and Miller, R.**,"Moving Finite Elements Part I" SIAM J. Numer. Anal. (1981)

[24] **Miller, K.**,"Moving Finite Elements Part II" SIAM J. Numer. Anal. (1981) pp 1019-1057

[25] **Miller, K.**,"Recent Results on FEM with Moving Nodes" in Accuracy

Estimates and Adaptive Refinements in Finite Element Computations (1986), John Wiley & Sons Ltd.

[26] **Adjerid, S. and Flaherty, J.E.**,"A Moving Mesh FEM with Local Refinement for Parabolic PDEs" Comp. Meth. Appl. Mech. Engrg. 55 (1986) pp 3-26

[27] **Oden, J.T.,Demkowicz, L.,Strouboulis, T. and Delvoo, P.**,"Adaptive Methods for Problems in Solid and Fluid Mechanics" in Accuracy Estimates and Adaptive Refinements in Finite Element Computations (1986), John Wiley & Sons Ltd.

[28] **Demkowicz, L. and Oden, J.T.**,"An Adaptive Characteristic Petrov-Galerkin FEM for Convection-Dominated Linear and Nonlinear Parabolic Problems in two space variables" Comp. Meth. Appl. Mech. Engrg. 59 (1986) pp 63-87

[29] **Oden, J.T.,Strouboulis, T. and Delvoo, P.**,"Adaptive FEM for the analysis of Invscid Compressible Flow : Part I,Fast Refinement/Unrefinement and Moving Mesh Methods for Unstructured Meshes" Comp. Meth. Appl. Mech. Engrg. 59 (1986) pp 327-362

[30] **Strouboulis, T. and Delvoo, P. and Oden,J.T.**, "A Moving-Grid Finite Element Algorithm for Supersonic Flow Interaction between Moving Bodies" Comp. Meth. Appl. Mech. Engrg. 59 (1986) pp 235-255

[31] **Oden, J.T.,Strouboulis, T.,Delvoo, Ph. and Howe, M.**,"Recent Advances in Error Estimation and Adaptive Improvement of FE Calculation"

[32] **Hughes, T.J.R. and Hulbert, G.M.**, "Space-Time Finite Element Methods for Elastodynamics : Formulations and Error Estimates" Comp. Meth. Appl. Mech. Engrg. 66 (1988) pp 339-363

[33] **Babuska, I.,Zienkiewicz, O.C.,Gago, J. and Oliveira, A. eds.**, Accuracy Estimates and Adaptive Refinements in Finite Element Comptations (1986), John Wiley & Sons Ltd.

[34] **Babuska, I.,Chandra, J. and Flaherty, J. eds.**, Adaptive Computational Methods for PDEs (1983)

[35] **Balas, M.J.**,"The Galerkin Method and Feedback Control of Linear Distributed Parameter Systems" J. Math. Anal. Appl. 91 (1983) pp 527-546

[36] _____,"Toward a practical control theory for distributed parameter systems in control and dynamic systems : Advances in Theory and Applications" Leondes ed. vol.18 Academic Press (1982) pp 361-421

[37] **Hughes, P.C.,**"Space Structure Vibration Modes : How many exist? Which modes are important?" IEEE Control Systems Magazine (1987)

[38] **Hu, A. and Skelton, R.E. ,**"Convergence Properties of Modal Costs for Certain Distributed Parameter Systems" ASME Vibration Conference Proc., Boston (1987)

[39] **Hu, A.,Skelton, R.E. and Yang, T.,**"Modeling and Control of Beam-like Structure" J. Sound and Vibration (1987)

[40] **Díaz, A.R., Jayasuria, S. and Kim, Y.J.,** "On the design of Nonlinear Controllers for Distributed Parameter Systems using Adaptive Finite Elements" Midwest Mechanics Conference (1987)

[41] **Kikuchi, Noboru,** Finite Element Methods in Mechanics Cambridge Univ Press (1986)

[42] **The Texas Finite Element Series** Prentice Hall
Vol 1 Finite Elements : An Introduction
Vol 2 Finite Elements : A Second Course
Vol 3 Finite Elements : Computational Aspects

[43] **Hughes, T.J.R.,** The Finite Element Method : Linear Static and Dynamic Finite Element Analysis Prentice-Hall (1987)

[44] **Strang, G. and Fix, G.,** An Analysis of the Finite Element Method Prentice-Hall (1973)

[45] **Ciarlet, P.G.,** The Finite Element Method for Elliptic Problems North-Holland (1978)

[47] **Melosh, R.J.,** "Finite Element Approximations in Transient Analysis" The Journal of the Astronautical Sciences, Vol XXXI, No. 3, PP 343-358 (1983)

[48] **Sun, C.T. and Huang, S.N.,** "Transverse Input Problems by Higher order Beam Element" Computers and Structures 5, pp 297-303 (1975)

[49] **Meirovitch, Leonard ,** Analytical Methods in Vibration The Macmillan Company (1967)

APPENDICES

Appendix A .

Mathematical Background [42,43]

A.1 Real Linear Space

A real linear space is a collection of objects for which the operations of addition and scalar multiplication are defined and behave as follows:

if x and y are members of the linear space and α and β are scalars, then $\alpha x + \beta y$ is also a member of the linear space.

Linear spaces may be endowed with important structures, most significantly, inner products and norms.

Definitions

An inner product (.,.) on a real linear space A is a map (.,.) : AxA $\rightarrow$ **R** with the following properties:

Let $x,y,z \in A$ and $\alpha \in \mathbf{R}$, then

1. $(x,y)=(y,x)$ (symmetry)
2. $(x+y)=(y+x)$ (linearity)
3. $(x+y,z)=(x+z)+(y+z)$
4. $(x,x) \geq 0$ (positive definiteness)

   $(x,x)=0$ if and only if $x=0$

A <u>norm</u> $||.||$ on a linear space A is a map $||.||: A \to \mathbb{R}$, with the following properties:

Let $x,y \in A$ and $\alpha \in \mathbb{R}$, then

1. $||x|| \geq 0$ and

   $||x|| = 0$ if and only if $x = 0$ (positive definiteness)

2. $||\alpha x|| = |\alpha| \, ||x||$

3. $||x+y|| \leq ||x|| + ||y||$ (triangular inequality)

A <u>semi-norm</u> $|.|$ on a linear space A is a map $|.|: A \to \mathbb{R}$ with the following properties :

Let $x,y \in A$ and $\alpha \in \mathbb{R}$, then

1. $|x| \geq 0$ (positive semi-definiteness)

2. $|\alpha x| = |\alpha||x|$

3. $|x+y| \leq |x| + |y|$ (triangular inequality)

A.2 The Continuity Class $C^m(\Omega)$

Suppose that Ω is a bounded region in $\mathbb{R}^2$, and that u is a given real-valued function of position in Ω. Then u is said to be the class of $C^m(\Omega)$ on Ω if u and all of its partial derivatives up to order m (m is nonnegative integer) are continuous at every point in Ω, i.e.,

$$C^m(\Omega) = \{ v \mid \frac{\partial^r v}{\partial x^i \, \partial y^j} \text{ is continuous in } \Omega \subset \mathbb{R}^2 \}$$

$$i,j \geq 0 \ , \ i+j = r \ , \ r \leq m$$

The class $C^m(\Omega)$ is a linear space of functions.

A.3 The $L^2(\Omega)$ Class

The function f is said to be in L^2 class if its derivatives can be defined only in a square integral sense. The function f in L^2 class will have the property of $\int_\Omega f^2 d\Omega < \infty$.

A.4 The Sobolev Class $H^m(\Omega)$

A function u is in $H^m(\Omega)$ if u and all of its partial derivatives of up to order m (nonnegative integer) are members of $L^2(\Omega)$, i.e. ,

$$H^m(\Omega) = \{ v \mid v, \frac{\partial v}{\partial x}, \frac{\partial v}{\partial y}, \ldots, \frac{\partial^m v}{\partial y^m} \in L^2(\Omega) \}$$

The space $H^m(\Omega)$ is a Hilbert space. The $H^m(\Omega)$ inner product, norm, and semi-norm are defined by

$$(u,v)_m = \{ \int_\Omega \sum_{\alpha+\beta \le m} [\frac{\partial^\alpha u}{\partial x^\alpha} \frac{\partial^\beta v}{\partial y^\beta}]^2 dx \}^{1/2} \qquad (H^m \text{ inner product})$$

$$||u||_m = (u,u)_m^{1/2} \qquad (H^m \text{ norm})$$

$$|u|_m = \{ \int_\Omega \sum_{\alpha+\beta=m} [\frac{\partial^{(\alpha+\beta)} u}{\partial x^\alpha \partial y^\beta}]^2 dx \}^{1/2} \qquad (H^m \text{ semi-norm})$$

where α and β are nonnegative integers.

A.5 Equivalence of Two Norms

Two norms, $||.||^{(1)}$ and $||.||^{(2)}$, on a linear space A, are said to be equivalent if there exist constants c_1, c_2 such that

$$c_1||x||^{(1)} \leq ||x||^{(2)} \leq c_2||x||^{(1)} \qquad \text{for all } x \in A$$

Appendix B .

Interpolation Functions for Quintic Beam Elements

B.1 Quintic Element Type 1 (3 nodes, 2 dof/node)

We list here interpolation functions for the quintic beam element with 3 nodes and 2 degrees of freedom per each node. A model of N quintic elements has a total 2(2N+1) degrees of freedom. This element has continuity in displacements and slopes (1st derivative) over the domain. Moments (2nd derivative) and shear forces (3rd derivative) are, however, discontinuous at element boundaries. The 5th order polynomial interpolation functions of this quintic element can be constructed using continuity conditions of displacement and slope at three nodes.

Interpolation functions for this element are as follows :

$$N_1(\eta) = 1 - 23\,\eta^2 + 66\,\eta^3 - 68\,\eta^4 + 24\,\eta^5$$

$$N_2(\eta) = L_K(\,\eta - 6\,\eta^2 + 13\,\eta^3 - 12\,\eta^4 + 4\,\eta^5\,)$$

$$N_3(\eta) = 16\,\eta^2 - 32\,\eta^3 - 16\,\eta^4$$

$$N_4(\eta) = L_K(\,-8\,\eta^2 + 32\,\eta^3 - 40\,\eta^4 + 16\,\eta^5\,)$$

$$N_5(\eta) = 7\,\eta^2 - 34\,\eta^3 + 52\,\eta^4 - 24\,\eta^5$$

$$N_6(\eta) = L_K(- \eta^2 + 5 \eta^3 - 8 \eta^4 + 4 \eta^5).$$

B.2 Quintic Element Type 2 (2 nodes, 3 dof/node)

Another type of quintic element can also be defined using 2 nodes and 3 degrees of freedom per node. A model of N quintic elements has a total 3(N+1) degrees of freedom. The difference between the quintic element type 1 and type 2 is the following: In the quintic element type 1, the displacement and slope (up to 1st derivative) are continuous across elements, and the moment (curvature, 2nd derivative) is discontinuous at element boundaries. However, in the quintic element type 2, the moment (curvature, up to 2nd derivatives) is also continuous at element boundaries. This type of quintic element has proven to be very efficient in the dynamical analysis of beam-like structures [48].

Interpolation functions for this type of element are as follows:

$$N_1(\eta) = 1 - 10 \eta^3 + 15 \eta^4 - 6 \eta^5$$

$$N_2(\eta) = L_K(\eta - 6 \eta^3 + 8 \eta^4 - 3 \eta^5)$$

$$N_3(\eta) = L_K^2(0.5 \eta^2 - 1.5 \eta^3 + 1.5 \eta^3 - 0.5 \eta^5)$$

$$N_4(\eta) = 10 \eta^3 - 15 \eta^4 + 6 \eta^5$$

$$N_5(\eta) = L_K(-4 \eta^3 + 7 \eta^4 - 3 \eta^5)$$

$$N_6(\eta) = L_K^2(0.5\ \eta^3 - \eta^4 + 0.5\ \eta^5)$$

Appendix C .

Exact Eigenpairs of a Uniform, Bernoulli-Euler Beam

The equation of motion of a uniform, Bernoulli-Euler beam of length ℓ can be written as

$$EI\frac{\partial^4 y(x,t)}{\partial x^4} + m\frac{\partial^2 y(x,t)}{\partial t^2} = 0 \qquad t \geq 0\ ,\ 0 < x < \ell \qquad (C.1)$$

where E,I,m are constants. The assumption that the solution to (c.1) is separable in time and space, i.e., $y(x,t)=u(x)T(t)$, leads to the eigenvalue problem of the following form : (see chapter 3)

$$\frac{d^4 u}{dx^4} - \beta^4 u = 0 \qquad (C.2)$$

where $\beta^4 = \frac{\lambda m}{E I}$ and $\lambda = \omega^2$.

The general solution of eq (C.2) is expressed as

$$u(x) = c_1 \sin \beta x + c_2 \cos \beta x + c_3 \sinh \beta x + c_4 \cosh \beta x \qquad (C.3)$$

C.1 Pinned-Pinned Beam (SS-SS)

The n-th mode eigenvalue can be found from

$\sin \beta\ell = 0$ or $\beta_n \ell = n\pi$ where $\beta^4 = \frac{\lambda m}{E I}$ or $\lambda = \beta^4 \frac{E I}{m}$

The corresponding eigenfunction $u_n(x)$ has the form of

$u_n(x) = c \sin \beta_n x$ where c is a arbitary constant.

C.2 Cantilever Beam (CL)

The n-th mode eigenvalue can be found from

$\cos \beta_n \ell \cosh \beta_n \ell = -1.$

The corresponding eigenfunction $u_n(x)$ is

$$u_n(x) = c [(\sin \beta_n \ell - \sinh \beta_n \ell)(\sin \beta_n x - \sinh \beta_n x) + (\cos \beta_n \ell + \cosh \beta_n \ell)(\cos \beta_n x - \cosh \beta_n x)]$$

C.3 Clamped-Pinned Beam (CL-SS)

$\tanh \beta_n \ell = \tan \beta_n \ell$

$$u_n(x) = c [(\cos \beta_n \ell - \cosh \beta_n \ell)(\sin \beta_n x - \sinh \beta_n x) - (\sin \beta_n \ell - \sinh \beta_n \ell)(\cos \beta_n x - \cosh \beta_n x)]$$

C.4 Clamped-Clamped Beam (CL-CL)

$\cos \beta_n \ell = \cosh \beta_n \ell$

$$u_n(x) = c [(\sin \beta_n \ell + \sinh \beta_n \ell)(\sin \beta_n x - \sinh \beta_n x) + (\cos \beta_n \ell - \cosh \beta_n \ell)(\cos \beta_n x - \cosh \beta_n x)]$$

C.5 Normalization

The exact eigenfunction should be normalized in an appropriate way, since the eigenfunction is unique up to scalar multiplications. The problem of comparing the exact solution to an approximate solution does not make sense if both functions are not normalized in a compatible way.

Usually, normalizations are performed with respect to the mass, i.e.,

$$\int_0^L u_n(x)\ m\ u_m(x)\ dx = \delta_{mn} \quad \text{or,}$$

assuming m=1 along the beam,

$$\int_0^L u_n(x)\ u_m(x)\ dx = \delta_{mn}$$

In the present work, the following normalization is adopted.

$$\max_{0 \le x \le L} |u_n(x)| = 1$$

Numerical Data of Eigenvalues

In table C.1, the exact eigenvalues for the different boundary conditions are listed.

Table C.1 Exact Eigenvalues $\lambda_n \ell^4 \frac{m}{E I}$ where ℓ is length of beam

mode\bc	SS-SS	CL-F	CL-SS	CL-CL
1st mode	$(\pi)^4$	$(1.875)^4$	$(4.730)^4$	$(3.927)^4$
2nd mode	$(2\pi)^4$	$(4.694)^4$	$(7.853)^4$	$(7.069)^4$
3rd mode	$(3\pi)^4$	$(7.855)^4$	$(10.996)^4$	$(10.210)^4$
4th mode	$(4\pi)^4$	$(10.995)^4$	$(14.137)^4$	$(13.352)^4$
5th mode	$(5\pi)^4$	$(14.137)^4$	$(17.279)^4$	$(16.493)^4$
6th mode	$(6\pi)^4$	$(17.279)^4$	$(20.420)^4$	$(19.635)^4$
7th mode	$(7\pi)^4$	$(20.420)^4$	$(23.562)^4$	$(27.776)^4$